Accepted Manuscript

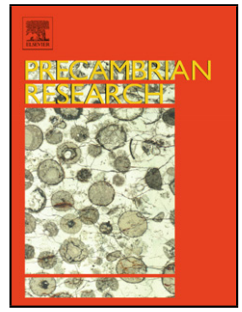

Title: Paleoproterozoic mafic dyke swarms from the Dharwar craton; paleomagnetic poles for India from 2.37-1.88 Ga and rethinking the Columbia supercontinent

Author: Mercedes E. Belica Elisa J. Piispa Joseph G. Meert Lauri J. Pesonen Jüri Plado Manoj K. Pandit George D. Kamenov Matthew Celestino

PII:	S0301-9268(13)00374-4
DOI:	http://dx.doi.org/doi:10.1016/j.precamres.2013.12.005
Reference:	PRECAM 3886

To appear in: *Precambrian Research*

Received date:	15-4-2013
Revised date:	28-9-2013
Accepted date:	5-12-2013

Please cite this article as: Belica, M.E., Piispa, E.J., Meert, J.G., Pesonen, L.J., Plado, J., Pandit, M.K., Kamenov, G.D., Celestino, M.,Paleoproterozoic mafic dyke swarms from the Dharwar craton; paleomagnetic poles for India from 2.37-1.88 Ga and rethinking the Columbia supercontinent, *Precambrian Research* (2013), http://dx.doi.org/10.1016/j.precamres.2013.12.005

Paleoproterozoic mafic dyke swarms from the Dharwar craton; paleomagnetic poles for India from 2.37-1.88 Ga and rethinking the Columbia supercontinent

Belica, Mercedes E.[a], Piispa, Elisa, J.[b], Meert, Joseph G.[a], Pesonen, Lauri J. [c], Plado, Jüri [d], Pandit, Manoj K.[e], Kamenov, George D.[a], Celestino, Matthew[a]

[a]Department of Geological Sciences, University of Florida, 241 Williamson Hall, Gainesville, FL 32611, USA

[b]Department of Geological and Mining Engineering and Sciences, Michigan Technological University, Houghton, 1400 Townsend Drive, MI 49931, USA

[c]Department of Physics, Division of Geophysics and Astronomy, PB 64, FI-00014 University of Helsinki, Helsinki, Finland

[d]Department of Geology, University of Tartu, Ravila 14A, 50411 Tartu, Estonia

[e]Department of Geology, University of Rajasthan, Jaipur 302004, Rajasthan, India

Corresponding author:

**Mercedes Elise Belica,*
e-mail: sadiebelica@gmail.com
Phone No. : +61 0458729951

Abstract

Here we report new paleomagnetic and geochronologic results from the Dharwar craton (south India) from 2.37-1.88 Ga. The presence of a ~85,000 km^2 radiating dyke swarm with a fanning angle of 65° is confirmed within Peninsular India at 1.88 Ga. North of the Cuddapah basin the dykes are oriented NW-SE and progress to an E-W orientation further south, converging at a focal point southeast of the basin. The Grand Mean dual polarity paleomagnetic pole falls at 36.5°N and 333.5°E (D=129.1º, I=4.2º, α95=4.5°, λ=2.1º) for 29 sites from the present study combined with previously published sites. Our continental reconstruction for India at ~1.9 Ga conflicts with the archetypal Columbia model, suggesting that the exact configuration needs modification. We also report two separate paleomagnetic directions from NW-SE (D=3.2º, I=56.4º, α95=17.9°, λ=37º) and N-S (D=240.1º, I=-65.5º, α95=10.9°, λ=47.7º) trending ~2.2 Ga dykes. We attribute this difference in directions to the separate magmatic pulses at 2.18 and 2.21 Ga identified by French and Heaman (2010). Our results place India at intermediate latitudes from 2.21-2.18 Ga and are supported by a positive baked contact test. New paleomagnetic results from E-W and NW-SE trending 2.37 Ga dykes, combined with previous work in the Dharwar craton, yields a Grand Mean dual polarity paleomagnetic pole at 15.1°N and 62.2°E (A95=4.0°), placing India at polar latitudes (D=88.7°, I=-81.7°, α95=4.8°, λ=73.7°). Here we also report a shallow NE direction (D=52.2°, I=-1.5°, α95=6.3°) previously classified as a secondary magnetization from three dykes near the Cuddapah basin. A baked contact test and petrophysical analysis of two cross-cutting dykes supports a primary remanence. Finally we present a Paleoproterozoic Apparent Polar Wander Path (APWP) for the Dharwar craton, and examine paleogeographic relationships between India and other cratonic blocks for the 2.37-1.88 Ga time interval.

1. Introduction

Recent advances in paleotectonics indicate that Earth's history was punctuated by numerous supercontinental configurations (Columbia, Rodinia, Gondwana, Pangaea; Meert 2012; Li et al. 2008; Meert and Lieberman 2008; Rogers and Santosh 2002; Zhao et al. 2002; 2004; Hou et al. 2008; Pesonen et al. 2003, 2012). The general makeup of the most recent supercontinent, Pangaea, is well constrained from seafloor magnetic anomaly data, paleomagnetism, geology, and faunal evidence (Benton 2005), although there are still vigorous debates regarding the exact configuration (Domeir et al. 2012). Given the controversies surrounding the different Pangaea reconstructions, it is no surprise that establishing the makeup of earlier supercontinents is far more difficult. In part, this is due to the lack of adequate geologic, isotopic, geophysical and paleontological data (Meert 2001; Meert and Torsvik 2003; Li et al. 2008). In attempting to decipher past continental configurations using paleomagnetism, it is important to seek regions where unaltered sequences of igneous and sedimentary Precambrian rocks are preserved. Peninsular India is one such region, and previous work indicates a high potential for generating useful data from India that can be used in conjunction with other regions to produce paleogeographic maps for the Precambrian (see Pradhan et al. 2010; Piper 2010; Bispo-Santos et al. 2008; Pesonen et al. 2003; Hou et al. 2008; French et al. 2008; French and Heaman 2010; Zhao et al. 2002, 2004; Condie 2002a,b; Rogers and Santosh 2002; Buchan et al. 2000, 2009; Pisarevsky and Sokolov 1999; Elming et al. 2001; Salminen et al. 2009; Piispa et al. 2011).

In attempts to reconstruct previous Proterozoic supercontinents, geologists use geologic similarities and the alignment of features such as orogenic belts, dyke swarms, or rapakivi pulses in order to establish contiguity (Zhao et al. 2002, 2004); however, paleomagnetic techniques remain the only quantitative test of such reconstructions (Meert 2002). As an example, the geologic record present in Precambrian terranes suggests a major global rifting event from 2.2 to 2.0 Ga followed 100 million years later by global widespread orogenesis from 1.9-1.7 Ga (Zhao et al. 2002, 2004). The orogenic belts that formed during this event were used to generate a plausible supercontinental assemblage named Columbia (Fig. 1; Zhao et al. 2004; Rogers and Santosh 2002; Meert 2012). In spite of the fact that high quality paleomagnetic data are being generated more rapidly in recent years, there is no current consensus on the exact make-up and geometry of Columbia (Ernst and Srivastava 2008; Meert 2012, Zhang et al. 2012, Evans and Mitchell 2011).

In addition to paleomagnetic data, the Large Igneous Province (LIP) record is also used for continental reconstructions (Ernst and Srivastava 2008). LIPs are large volume and geologically brief magmatic events that typically occur in an intraplate setting and commonly accompany the rifting or assembling of supercontinents (Ernst and Srivastava 2008). A LIP typically has a focal point (plume source) that can be identified by the convergence of the associated radiating dyke swarms. Coeval radiating dykes can be used as piercing points between different continental nuclei, where the focus of each swarm overlaps in the correct reconstruction (Ernst and Srivastava 2008).

Mafic dykes are ideal for paleomagnetic studies because they cool rapidly and therefore provide an accurate, albeit instantaneous record of the Earth’s magnetic field (Tauxe 2010). In addition to being good recorders of the Earth’s magnetic field, techniques were developed recently to separate Uranium-bearing minerals from mafic dykes. These minerals (primarily zircon and baddeleyite) are used to establish the crystallization ages of the dykes (French and Heaman 2010; French et al. 2008; Pradhan et al. 2012; Pradhan et al. 2010; Halls et al. 2007).

Moreover, the primary nature of the remanent magnetization in dykes can be verified by (field tests, most notably) the baked contact test (Everitt and Clegg 1962). These favourable characteristics of mafic dykes have spurred a number of recent paleomagnetic studies that attempt to establish a well-dated emplacement age with a stable paleomagnetic direction in order to constrain better paleomagnetic poles for the Precambrian (Meert et al. 2011; Pradhan et al. 2008, 2010; Halls et al. 2007; French et al. 2008; French and Heaman 2010; Lubnina et al. 2010; Piispa et al. 2011; Pradhan et al. 2012).

Here we present new paleomagnetic and supplementary geochronologic data from Dharwar mafic dykes and the Pullivendla sill in southeastern peninsular India (Fig. 2). Sample areas included swarms located near Hassan, Tiptur and Kunigal (west of Bengaluru; Fig. 3) as well as a dense concentration of dykes in the Tirupati-Chittoor region (E-NE of Bengaluru; Fig. 3). Our new paleomagnetic results help refine the Apparent Polar Wander Path (APWP) for the Dharwar craton during the Paleoproterozoic, from about 2.37 Ga to 1.88 Ga. Implications for reconstructions during this interval will be discussed, and proposed supercontinent configurations will be evaluated using recent well-dated paleomagnetic poles and coeval magmatic events on other continents.

2. Regional Geology

Peninsular India consists of four distinct cratonic nuclei: the Banded Gneiss Complex-Bundelkhand craton in the northwest and central regions, the Bastar craton in the south-central region, the Singhbhum craton in the eastern region, and the Dharwar craton in the south (Fig. 2; Naqvi et al. 1974; Naganjaneyulu and Santosh 2010; Bandari et al. 2010; Meert et al. 2010). Peninsular India was assembled by the collision of these individual cratonic blocks along the Central Indian Tectonic Zone (CITZ) or the Satpura Belt, but the exact timing of the event is still debated. A number of Neoarchean to Proterozoic granitoids including the Closepet Granite (2.51 Ga) in the Dharwar craton, and the Berach Granite in the Aravalli craton (2.56-2.44 Ga), intrude the older basement gneisses and supracrustals (Meert et al. 2010; Wiedenbeck et al. 1996; Jayananda et al. 2000). Meert et al. (2010) suggested that the amalgamation of India's individual cratonic nuclei took place by the end of the Archean, and that the ~2.5-2.45 Ga intrusive granitoids mark a major stabilization phase for peninsular India. Others contend that this stabilization phase did not occur until 1.6 Ga (Yedekar et al. 1990; Roy and Prasad 2003; Roy et al. 2006; Bhandari et al. 2010). Even younger (1.1-1.0 Ga) ages reported for this collision may represent reactivation along this pre-existing zones of weakness from collisional events in the Eastern Ghats or Aravalli regions (Bhowmik et al. 2011; Singh et al. 2010; Bhowmik et al. 2012).

The Dharwar craton is bordered by the Deccan Traps to the north, the Eastern Ghats and the Godavari Rift to the east, the Arabian Sea to the west, and the Southern Granulite Terrane to the south (Rogers 1986; Naqvi and Rogers 1987). The Dharwar protocontinent consists of the Dharwar, Bastar, and Singhbhum cratons, and is separated from the northern Banded Gneiss Complex (Aravalli)-Bundelkhand protocontinent by the CITZ (French and Heaman 2010). The N-S trending 2.51 Ga Closepet Granite divides the Dharwar craton into eastern (EDC) and western (WDC) nuclei (Friend and Nutman 1991; Ramakrishnan and Vaidyanadhan 2008; Naqvi and Rogers 1987). Local basement rock includes 3.0-2.55 Ga granites and gneisses (EDC) as well as 3.4-2.7 Ga tonalite-trondhjemite gneisses (WDC; Jayananda et al. 2006; Balakrishnan et al. 1990; Vasudev et al. 2000; Chadwick et al. 2000; Chardon et al. 2002; Meert et al. 2010).

The southern peninsular region of India contains several intracratonic basins (Purana basins) that developed during the Paleo-Neoproterozoic (French et al. 2008). The largest of these is the crescent-shaped Cuddapah basin located in the EDC (Fig. 3). The basin spans an area of ~44,500 km^2 with a minimum total stratigraphic thickness of ~12 km (French et al. 2008; Nagaraja Rao et al. 1987; Ramam and Murty 1997; Singh and Mishra 2002). It is composed of four sub-basins: the Papaghani, the Kurnool, the Srisailam, and the Palnad basins (Nagaraja Rao et al. 1987). The Papaghani sub-basin is located in the western segment of the Cuddapah basin (Fig. 3) and contains several robust ages that help constrain sedimentation and magmatism (Bhaskar Rao et al. 1995; Anand et al. 2003). The Gulcheru Formation quartzite is the lowest unit within the basin; it rests nonconformably on the underlying basement rocks of the Dharwar craton (French et al. 2008; Nagaraja Rao et al. 1987; Murty et al. 1987). The age of the underlying peninsular gneiss is constrained from dating of the Closepet Granite (2.51 Ga; Friend and Nutman 1991; Jayananda et al. 1995). Above the Gulcheru quartzite lies the stromatolite-bearing dolomitic limestone, chert, and shale of the Vempalle Formation. Interbedded mafic sills and basaltic lava flows are also present near the top of this section (Saha and Tripathy 2012). An unconformity rests between the Vempalle Formation and the Pullivendla quartzite of the overlying Tadpatri Formation. The Tadpatri Formation contains numerous dolerite, basaltic, and picrite sills within the surrounding sedimentary rocks (Saha and Tripathy 2012). One sill at the base of this formation (Pullivendla sill) has a well constrained U-Pb age of 1885 ± 3.1 Ma (French et al. 2008). This age provides a constraint for the underlying sedimentary layers (Papaghani Group >1900 Ma; Saha and Tripathy 2012). An elliptical positive gravity anomaly is present in the western segment of the Cuddapah basin and it parallels the NW-SE trending Papaghani sub-basin (Bhattacharji and Singh 1984). The southwest segment of the basin also contains the densest concentration of mafic sills and flows, indicating the presence of a lower-crustal lensoid mafic body (Bhattacharji and Singh 1984; Saha and Tripathy 2012). Widespread coeval magmatic events in the Bastar and Dharwar cratons as well as the Cuddapah basin lend evidence for a plume or mantle upwelling at ~1.9 Ga that may be the precursor to early extension within the Papaghani sub-basin, and possibly a site of continental breakup (see discussion; Saha and Tripathy 2012).

3. Previous work

The Indian cratons are cross-cut by numerous Precambrian mafic dyke swarms as well as sills and mafic-ultramafic intrusions (Ernst and Srivastava 2008). The Dharwar craton contains the densest concentration of these dykes (Fig. 3) and is central to numerous supercontinent reconstructions, so obtaining accurate emplacement ages for the dykes is essential for any paleomagnetic reconstruction (French and Heaman 2010). The dykes crosscut Archean granites and gneisses and have a wide variety of orientations (E-W, WNW-NW, NE-ENE, and N-S; Rao et al. 1995; French et al. 2008; French and Heaman 2010; Halls et al. 2007; Pradhan et al. 2010). Sections 3.1-3.3 of this manuscript review the characteristics and geochronology for each of the Paleoproterozoic dyke swarms. A combined list of previously published (and unpublished) paleomagnetic directions and relevant statistics is provided in Tables 1-3.

3.1. 2.37 Ga dykes

The Dharwar giant dyke swarm (Bengaluru swarm) contains several precise U-Pb ages of 2367 ± 1 Ma (Yeragumballi diabase dyke, baddeleyite; Halls et al. 2007), 2365.4 ± 1.0, 2365.9 ± 1.5 and 2368.6 ± 1.3 Ma (Harohalli, Penukonda, and Chennekottapalle dykes, baddeleyite; French and Heaman 2010), as well as 2368.5 ± 2.6 Ma and 2367.1 ± 3.1 Ma (Karimnagar dykes, baddeleyite; Kumar et al. 2012a). This predominately E-W trending swarm is at least 300 km wide and 350 km long, consists mainly of iron-rich tholeiite, and was emplaced fairly rapidly (~5 Myr; Kumar et al. 2012a; Ernst and Srivastava 2008). Paleomagnetic directions from the dykes have a characteristic steep remanence that has been regarded as primary from a positive baked contact test (Kumar and Bhalla 1983); however, new sampling from the same cross-cutting dykes gives different results (This study; see sections 5.4 and 6.4). It has been suggested that the dykes associated with this magmatic event are part of a radiating swarm, with a focal point west of the present day craton boundary (Kumar et al. 2012a). The hypothesis is based on a variance in dyke trend where the majority of dykes to the south trend E-W, and dykes to the north, just south of the Godavari rift, trend roughly NE. Another possibility is that the dykes are part of a linear E-W trending swarm with some tectonic complications at the northern end. The NW-SE trending Mesoproterozoic (1600-1500 Ma; Chaudhuri and Deb 2004) Pranhita-Godavari Basin records a major period of northeast crustal extension within Peninsular India and is located just north of the NE trending dykes. The main period of crustal extension began in the early Permian during pre-breakup of Gondwana, followed by episodic rifting in the late Permian through Cretaceous (Biswas 2003). The extension associated with this rift may have caused a rotation of Paleoproterozoic dykes in the vicinity. Differential extension along the rift would rotate E-W dykes into a NE orientation if extension was greatest along the northwest segment of the rift; however, more structural research in the area is needed to support this hypothesis.

3.2. 2.21-2.18 Ga dykes

Northwest trending dykes of the 2180 Ma Mahbubnagar swarm are mainly gabbro, dolerite, and metapyroxenite, and geochemically tholeiitic and sub-alkalic and quartz or olivine normative (Ernst and Srivastava 2008; Pandey et al. 1997). It has been suggested that the dykes are fairly widespread throughout the Dharwar craton, and recent U-Pb ages indicate the presence of two large (100,000 km^2) dyke swarms, the first at 2.21 Ga (mainly N-S) and the second at 2.18 Ga (NW-SE and E-W), with a possible convergence point west of the Deccan Flood basalt province (French and Heaman 2010). The NW-SE trending Somala dyke and NNW-SSE Kandlamadugu dyke have baddeleyite ages of 2209.3 ± 2.8 Ma and 2220.5 ± 4.9 Ma, and the E-W trending Bandapalem dyke and NW-SE trending Dandeli dyke have ages of 2176.5 ± 3.7 Ma (baddeleyite and zircon) and 2180.8 ± 0.9 Ma (baddeleyite). A stationary and long-lived mantle plume may explain this protracted period of magmatism (35 Ma), and could be associated with the breakup of an Archean-Paleoproterozoic continent (French and Heaman 2010). Additional ages of 2173 ± 43 Ma and 2190 ± 51 Ma (Sm-Nd; Kumar et al. 2012b) as well as 2215.2 ± 2.0 and 2211.7 ± 0.9 Ma (U-Pb, baddeleyite; Srivastava et al. 2011) confirm that the 2.21 Ga dykes are part of a 450 km long N-S trending swarm shown to be fairly chemically homogenous (Kumar et al. 2012b). Kumar et al. (2012b) presented a preliminary paleomagnetic analysis of 3 dykes, covering a 350 km long outcrop; however, the pole has not yet been confirmed as primary. Preliminary paleomagnetism of NW and E-W trending dykes belonging to the ~2.18 magmatic pulse will be presented here (see results and discussion).

3.3. 1.88 Ga dykes

Recent work within the Dharwar and Bastar cratons has hinted at the presence of a remnant Large Igneous Province (LIP) at 1.88 Ga. French et al. (2008) obtained high precision U–Pb dates of 1891.1 ± 0.9 Ma (baddeleyite) and 1883.0 ± 1.4 Ma (baddeleyite and zircon) for two NW-SE trending mafic dykes from the BD2 dyke swarm in the Southern Bastar craton, as well as an age of 1885 ± 3.1 Ma for the Pullivendla mafic sill within the Cuddapah basin. These ages indicate that magmatism spanned at least 10 million years (French et al. 2008). French et al. (2008) informally named this magmatic event the Southern Bastar-Cuddapah large igneous province, and speculated that this event spanned a wide area of cratonic India. The dykes trend NW-SE and E-W and consist of sub-alkaline basalts, ranging from quartz-normative tholeiites, with subordinate olivine- and nepheline-normative tholeiites (French et al. 2008; Ramchandra et al. 1995). The presence of 1890 Ma magmatism on both the Bastar and Dharwar cratons indicates that the two blocks were in close proximity at this time (see results).

Ernst and Srivastava (2008) linked 1.88 Ga NW-SE trending dykes in the Bastar craton (French et al. 2008) with an E-W trending dyke west of the Cuddapah basin (Halls et al. 2007) and speculated that a major radiating dyke swarm could be present within the Dharwar craton, with a convergence point east of the craton boundary. This focal point may mark the position of an 1890 Ma mantle plume (see discussion). Mafic magmatism at 1.88 Ga is common on other Precambrian cratons worldwide, including the Superior, Slave, Kaapvaal, Siberian, and possibly East European cratons (Ernst and Srivastava 2008; French et al. 2008). The global distribution of 1.88 Ga intracratonic mafic magmatism likely indicates a period of either enhanced mantle plume activity or a large scale upwelling event that affected extensive regions of the Earth's mantle (French et al. 2008). This magmatism may have been accompanied by the development of several intracratonic basins in the Dharwar protocontinent, including the Abujhmar and Cuddapah basins (French et al. 2008).

Meert et al. (2011) presented a preliminary paleomagnetic analysis of five 1.88 Ga Bastar mafic dykes within the Keskal dyke swarm, and found a dual polarity magnetization with a NW-SE declination and shallow inclination. The paleomagnetism is in agreement with previous studies on the Cuddapah Traps volcanics (Clark 1982) and an E-W dyke adjacent to the Cuddapah basin (Kumar and Bhalla 1983), indicating that they may be part of the same 1.88 Ga dyke swarm (French et al. 2008; Meert et al. 2011).

4. Methods

4.1. Paleomagnetism

Eighty seven sites were sampled for paleomagnetic analysis with a total of ~870 core specimens from the mafic dykes intruding the Dharwar craton. Samples were drilled in the field using a portable gasoline-powered hand drill or taken as oriented hand samples. The samples were oriented using a Brunton magnetic compass as well as a solar compass to correct for any magnetic interference and local magnetic declination. The location, size, orientation, and quality of each outcrop were recorded, and where the geology allowed, baked contact samples were collected from the regional basement gneisses or granites. Typically we drilled several cores within the baked zone (~half-width of the dyke), several cores from the hybrid zone, and where needed, several from the unbaked host rock. Samples were returned to the University of Florida or University of Helsinki, where they were cut (or drilled and cut) into standard-sized cylindrical specimens of relatively equal volume, and natural remanent magnetization (NRM) was measured on either a Molspin spinner magnetometer or a 2-G cryogenic magnetometer. Preliminary pilot samples (2 cores from each site) were stepwise treated using thermal or alternating field demagnetization and the most effective demagnetization method and steps were chosen for each site based on the preliminary evaluation of these samples. Alternating field demagnetization was carried out using a home-built AF demagnetizer with fields up to 150 mT (University of Florida) or with a 2G AF demagnetizer (University of Helsinki), while thermal demagnetization was conducted using an ASC-Scientific TD-48 thermal demagnetizer up to temperatures of 600°C. Linear segments of the resulting demagnetization paths were analyzed through principal component analysis (Kirschvink 1980) and great circle paths using Super IAPD software (Torsvik et al. 2000).

4.1.1. Rock Magnetic Experiments

Curie temperature experiments were conducted on one powdered sample from each site in order to identify the magnetic carriers present in the dykes. Experiments were conducted with a KLY-3S susceptibility bridge adapted with a CS-3 heating unit, and susceptibility was measured incrementally during the heating and cooling of the samples. Susceptibility vs. temperature was plotted and heating and cooling Curie temperatures were calculated using the Cureval8 software (M. Chadima & V. Jelinek 2012). Isothermal remanent magnetization (IRM) studies were carried out on an ASC Scientific Model IM-10-30 impulse magnetizer for selected samples in order to further characterize the magnetic carriers. Backfield IRM was also performed on previously AF-demagnetized cores to obtain the remanence coercivity.

4.2. Geochronology

Samples from the NW-SE and E-W trending dykes were processed for geochronology (Fig. 4). Each sample was pulverized and the zircons were isolated using conventional methods of mineral extraction and gravity and magnetic separation techniques at the University of Florida. Each sample was crushed, disk milled, and sieved to a < 250 μm grain size fraction. Heavy liquid mineral separation with multiple agitation periods was used to isolate grains in the higher density fractions. Samples were then repeatedly passed through a Frantz Isodynamic Magnetic Separator up to a current of 1.2 A (10° tilt). Two euhedral zircon grains were handpicked from the remaining sample using an optical microscope, and were mounted in resin and polished to expose the medial sections. The plugs were further cleaned in 5% nitric acid to remove common-Pb surface contamination. U-Pb isotopic analyses were conducted at the Department of Geological Sciences (University of Florida) on a Nu Plasma multicollector plasma source mass spectrometer equipped with three ion counters and 12 Faraday detectors. The LA–ICPMC–MS is equipped with a specially designed collector block for simultaneous acquisition of ^{204}Pb (^{204}Hg), ^{206}Pb and ^{207}Pb signals on the ion-counting detectors and ^{235}U and ^{238}U on the Faraday detectors (Mueller et al. 2008). Mounted zircon grains were laser ablated using a New-Wave 213 nm ultraviolet laser beam. During U-Pb analyses, the sample was decrepitated in a He stream and then mixed with Ar-gas for induction into the mass spectrometer. Background measurements were performed before each analysis for blank correction and contributions from ^{204}Hg. Each sample was ablated for ~30 s in an effort to minimize pit depth and fractionation. Data calibration and drift corrections were conducted using the FC-1 Duluth Gabbro zircon standard, and long term reproducibility was 2% for $^{206}Pb/^{238}U$ (2σ) and 1% for $^{207}Pb/^{206}Pb$ (2σ) ages (Mueller et al. 2008). Data reduction and correction were conducted using a combination of in-house software and Isoplot (Ludwig 1999).

4.3. Ground Magnetic Mapping

To reveal the age relationship between the ENE-trending TN and NNW-trending TP cross-cutting dykes we conducted a ground magnetic survey at the intersection area in Tippanapalle (Fig. 5). The survey was carried out by measuring the total magnetic field strength (accuracy 0.5 nT) using a proton precession magnetometer (G-856 by Geometrics, Inc.). The raw datum was corrected against diurnal variations that were repeatedly measured in three control points. Samples were also collected from both dykes on each side of the intersection point for petrophysical and paleomagnetic analysis (Fig. 5a).

5. Results

Five different paleomagnetic directions were isolated from the dataset (59 sites), and several of these directions have been previously identified and reported in the literature (Halls et al. 2007; French and Heaman 2010; Piispa et al. 2011; Kumar et al. 2012a; Kumar et al. 2012b; Meert et al. 2011; Clark 1982; Hargraves and Bhalla 1983; Kumar and Bhalla 1983; Bhalla et al.

1980; Prasad et al. 1984). Here we group our results by each swarm using known directional data, samples from rocks with reported ages, and new directional data.

5.1. 2.37 Ga dykes

Eighteen E-W, NW-SE, and NE-SW trending dykes (Table 1) have paleomagnetic directions with NRM intensities ranging from 0.12 to 9 A/m. Representative demagnetization behaviour is displayed in Figures 6a and b. Thermal demagnetization revealed unblocking temperatures between 550° and 570°C (Figs. 6a and b), and alternating field treatments show median destructive fields of 40 to 70 mT. Unblocking temperatures in this range are consistent with that of magnetite (Butler 2004). Samples from sites 14, 39, and 45 show a sharp drop in intensity (<50%) near 320°C upon heating, indicating the presence of pyrrhotite (Fig. 6a). Representative results of thermomagnetic analysis are shown in Figure 7a. Curie temperature experiments (susceptibility vs. temperatures) reveal nearly reversible heating and cooling curves with a single magnetic phase. Sites 14, 39, and 45 reveal two magnetic phases, with a sharp decrease in susceptibility at ~320°C (pyrrhotite), and a larger drop by ~565°C (magnetite; Butler 2004). The heating Curie temperature Tc_H from Site 62 is 563.8°C and the cooling Curie temperature Tc_C is 557.7°C (Fig. 7a). IRM curves reveal magnetic saturation between 0.2 and 0.3 T and backfield coercivity of remanence ranged from 0.08 to 0.12 mT. These values are consistent with magnetite as the main magnetic carrier. Figure 8a displays IRM curves for sites 16 and 62, with magnetic saturation values of 0.1 and 0.15 T, and backfield coercivity remanence values of 0.1 and 0.12 mT.

The majority of dykes revealed a stable uni-vectorial demagnetization trend during both treatments, with four dykes containing multicomponent directions. The main direction is carried by the highest coercivity and unblocking temperature. The direction is distinguished by a steep negative or positive inclination previously recognized and precisely dated (Halls et al. 2007; French and Heaman 2010; Piispa et al. 2011; Kumar et al. 2012a; Figs. 6a and b). These dykes are part of the 2.37 Ga E-W trending Dharwar giant dyke swarm (Bengaluru swarm) and have a declination=65°, and an inclination=-81.7° (α95=8.3°) calculated using a common site location. Our results confirm the large geographic extent of this swarm within southern peninsular India (Halls et al. 2007; Kumar et al. 2012a). The dykes have a dual polarity magnetization with a mean normal pole at 14.8°N and 60.2°E (α95=5.2°), and a mean reverse pole at 15.9°N and 69.9°E (α95=12.3°). A reversal test was conducted to test antipodality of the means and resulted in a classification of R_b (observed λ=9.66, Critical λ=12.36; McFadden and McElhinny 1990). The dykes have an overall mean paleomagnetic pole (mean for all sites in the present study) at 6.6°N and 63.1°E (A95=8.3°) and a combined Grand Mean pole (mean for all published sites combined with the present study) at 15.1°N and 62.2°E (A95=4.0°). The combined dataset is restricted to sites with α95≤20° and N≥3. Using Google Earth, dyke characteristics (trend, width, rock type, grain size), and matching paleomagnetic directions, we also calculated a combined mean pole for the Great dyke of Penukonda (sites ii, P28, 71, 596, and BU; Table 1). A primary remanence for 2.37 Ga dykes is supported by a positive baked contact test (Fig. 9a). At site 14, twelve samples were collected from the gneissic host rock at the contact, and three additional samples were collected from unbaked gneisses within the swarm. Dyke samples yielded a steep negative inclination (D=44.5°, I=-77.7°, α95 =2.9°), the baked gneiss samples yielded similarly steep inclinations (D=161.9°, I=-84.4°, α95=10°), whereas the unbaked gneiss yielded an intermediate and positive inclination (Fig. 9a). This represents the first successful baked contact test for this swarm (see sections 5.4 and 6.4 for discussion of Kumar and Bhalla 1983). The combined dataset for the 2.37 Ga dykes has a reliability criteria of Q=6 (Van der Voo 1990), and represents a robust paleomagnetic pole.

5.2. 2.21-2.18 Ga dykes

Nine dykes (Table 2) revealed paleomagnetic directions with NRM intensities ranging from 0.1 to 4.6 A/m. Representative demagnetization behaviour is displayed in Figures 6c and d. Unblocking temperatures were between 560° and 570°C for thermal treatments. Figure 6c (site 64) shows a ~70% decay in magnetic intensity near 320°C, indicating the presence of pyrrhotite. Curie experiments show reversible heating and cooling curves with one magnetic phase. The heating Curie temperature Tc_H for site 17 is 555.2°C, and the cooling Curie temperature Tc_C is 515°C (Fig. 7b). IRM curves reveal magnetic saturation between 0.2 and 0.25 T, along with a backfield coercivity of remanence value of 0.08 mT (Fig. 8b). Dykes reveal both stable uni-vectorial demagnetization trends (Fig. 6c) as well as multicomponent directions (Fig. 6d). Secondary components are removed by ~400°C.

Six of these dykes trend N-S, NE-SW and NW-SE and yielded either a west-southwest or east-northeast declination and a fairly steep inclination (D=236.1°, I=-67.2° α95=20.1°; calculated using a common site location). The direction is similar to results recently obtained from N-S trending dykes in the Dharwar craton (Kumar et al. 2012b) that have been identified as part of the 2.21 Ga large igneous province. The dykes have a dual polarity magnetization with a mean normal pole at 28.3°S and 306.6°E (α95=12.1°), and a mean reverse pole at 35.1°S and 287.5°E (α95=25.6°). The reversal test resulted with a classification of Rc (observed λ=17.58, Critical λ=29.99; McFadden and McElhinny 1990). The dykes have an overall mean paleomagnetic pole at 32°S and 297°E (A95=22°) and a combined Grand Mean pole at 30.8°S and 300.7°E (A95=11.5°; λ=47.7°). A combined mean pole was also calculated for the Great dyke of Closepet (AKLD, P24, 17, 20, and TP; Table 2). Although some of the dykes have been dated (U-Pb, 2215 ± 2.0 Ma; Srivastava et al. 2011), the magnetization has not been confirmed as primary due to the lack of an adequate baked contact test. This paleomagnetic direction also resembles a pole recently reported by Pisarevsky et al. (2013a) for the Lakhna dykes in the Bastar craton. The dykes have U-Pb zircon age of 1466 ± 2.6 Ma, and it is possible that the 2.21 Ga dykes may contain this direction as an overprint. We tentatively classify this group of Dharwar dykes to the 2.21 Ga swarm after Kumar et al. (2012b), but note the possibility of a secondary magnetization.

Four NW-SE and E-W trending dykes (including P10; Piispa et al. 2011) have a slightly different direction from the previous pole (Fig. 6d) with shallower positive inclinations and northerly declinations (D=3.2°, I=56.4°, α_{95}=17.9°; calculated using a common site location). These dykes were sampled from the 2.18 Ga Mahbubnagar swarm (U-Pb; French et al. 2004; Ernst and Srivastava 2008). A mean paleomagnetic pole of 67.5°N and 84.5°E (A_{95}=17.8°) was calculated for the 2.18 Ga dykes, with a corresponding paleolatitude of 37° (calculated using a common site location). A baked contact test for a dyke in the Mahbubnagar swarm (site 571) supports a primary magnetization (Fig. 9b). The mean dyke direction has a northerly declination and positive inclination (D=3°, I=45°, α_{95}=3.7°), the baked host gneiss has a northeast declination (D=23°, I=50.2°, α_{95}=10°), and the unbaked gneiss has a northwest and negative inclination (D=339°, I=-42°, α_{95}=7°).

5.3. 1.88 dykes

5.3.1. Geochronology

U-Pb ages from zircons were determined for the NW-SE trending dyke sample 1019 (site 19) from the Kunigal region. The dyke sample yielded several zircons suitable for U-Pb isotopic analysis; however only 2 of the zircons yielded useful data and the remainder were highly (>50%) discordant. Two of these zircons yielded $^{207}Pb/^{206}Pb$ ages of 1847 ± 6 Ma and 1839 ± 8 Ma (Fig. 4; Table 5). These represent minimum ages for the dyke and we note that paleomagnetic directions from this site and other well-dated 1.9 Ga dykes are in agreement, so these minimum ages are broadly consistent with recent geochronologic results reported for the NW striking Pullivendla sill (1885 ± 3.1 Ma; French et al. 2008) and NW-SE trending Bastar dykes (1891.1 ± 0.9 Ma and 1883.0 ± 1.4 Ma; French et al. 2008).

5.3.2. Paleomagnetism

Twenty eight NE-SW, E-W and NW-SE dykes (Table 3) and the Pullivendla sill have directions with NRM intensities ranging from 0.76 to 49 A/m. The dykes record a dual polarity magnetization, and representative demagnetization behaviour for both polarities is shown in Figures 10a-c. Thermal demagnetization revealed unblocking temperatures between 540° and 570°C indicative of magnetite (Figs. 10b and c), and alternating field treatments show median destructive fields of 40 to 70 mT (Fig.10a). Representative results of thermomagnetic analysis are shown in Figure 7c. Curie temperature experiments reveal two magnetic phases in 8 of the dykes. The first phase (associated with pyrrhotite) shows a sharp decrease in magnetic susceptibility near 320°C, and the second phase shows a much larger drop (associated with magnetite) at 545-563°C. Figure 7c (site 67) has a heating Curie temperature Tc_H of 555.8°C and a cooling Curie temperature Tc_C of 567.5°C. The bulge in the heating curve around 300°C indicates the presence of pyrrhotite. IRM curves reveal magnetic saturation values between 0.25 and 0.3 T, and backfield coercivity of remanence values between 0.05 and 0.1 mT (Fig. 8c).

The majority of the dykes revealed a stable univectorial demagnetization trend during thermal treatments, and five of the dykes reveal multicomponent directions. Secondary components are removed by 350°C (site 32) for thermal demagnetization and by 40 mT (site 40) for alternating field demagnetization. The main direction (D=129.3, I=9.2; calculated using a common site location) is carried by the highest coercivity and unblocking temperature, with either a northwest or southeast declination, and a shallow inclination (Fig. 10)

The mean paleomagnetic pole matches a preliminary pole from 1.88 Ga NW trending Bastar dykes (Meert et al. 2011), the Cuddapah Traps volcanics (Clark 1982), several E-W to NE trending dykes near the Cuddapah basin (Hargraves and Bhalla 1983; Kumar and Bhalla 1983; Radhakrishna et al. 2013) and near Tiptur (Bhalla et al. 1980), as well as Cuddapah basin sediments (Prasad et al. 1984). The dykes have a dual polarity magnetization with a mean normal pole at 27°N and 335.3°E (α95=10.4°), and a mean reverse pole at 38.6°N and 333.1°E (α95=5.0°; Fig. 11). A reversal test was conducted to test antipodality of the means and resulted in a classification of R_b (observed λ=9.42, Critical λ=11.94; McFadden and McElhinny 1990) for dykes with α95≤15. The dykes have an overall mean paleomagnetic pole at 35.9°N and 331.2°E (A95=6.6°) and a combined Grand Mean pole at 36.5°N and 333.5°E (A95=5.6°; λ=2.1°). A positive baked contact test at site UR supports a primary remanence (Fig. 9c). One contact amphibolite and seven unbaked amphibolite samples were collected at this site in addition to the dyke. The mean dyke direction is northwest and shallow (D=324.2° I=10.1°, α95=14.7°), the baked direction is also northwest and shallow (D=326.6°, I=-1.3°), and the unbaked direction has a very steep inclination (D=13.4° I=75.2°, α95=12°; Fig. 9c). The primary nature of this direction, three well constrained and consistent U-Pb ages, and a large, statistically significant paleomagnetic dataset (58 sites, α95=4.5°, Q=6; Van der Voo 1990) supports a robust paleomagnetic pole for the Dharwar craton at ~1.9 Ga.

5.4 Cuddapah swarm

Three NE-SW and E-W trending dykes located southwest of the Cuddapah basin revealed a distinctively different paleomagnetic direction (Table 4). Unblocking temperatures for the dykes were between 550° and 580°C, and alternating field treatments show median destructive fields of 30 to 60 mT. Dyke SC (NE-SW) has a stable and univectorial magnetization while SB (NE-SW) and MG (E-W) revealed multicomponent directions. The secondary components were removed by 300°C for thermal demagnetization and by 15 mT for alternating field demagnetization. The main direction is carried by the highest coercivity and unblocking temperature and reveals a shallow NE direction. Combining these three dykes with 14 other dykes around Cuddapah basin (Kumar and Bhalla 1983; Rao et al. 1990; Pradhan et al. 2010; Piispa et al. 2011; Radhakrishna et al. 2013b) yields a mean paleomagnetic direction of D=52.2° and I=-1.5° (α95=6.3°; calculated using a common site location). New mean directions from different studies on the same NE trending dykes near the town of Bukkapatnam (P27m+dyke iii and P29+dyke iv) were also calculated.

Two dykes previously studied by Kumar and Bhalla (1983) and Piispa et al. (2011) were chosen for baked contact tests due to the high quality of the outcrops (a river cut and a recent channel cut). Both baked contact tests were positive (Table 4), although we note that the number of baked and unbaked samples (one and one) at site P29 is statistically insufficient. At site P27m we report a positive baked contact test near the town of Bukkapatnam where two dykes crosscut one another (E-W trending Great dyke of Penukonda and NE trending dyke). Eight samples were collected across the width of the E-W dyke (Great dyke of Penukonda) with increasing distance to the approximate site of cross-cutting (Fig. 12a). Fourteen samples from the NE trending dyke (P27m) and four samples from the baked E-W trending dyke have a very similar shallow NE direction whereas the four baked samples show an increasingly steeper direction similar to that of the E-W dyke (Fig. 12b; Table 4). Additionally, sites 71 and BU (Table 1) of the Great dyke of Penukonda (~50 and ~150 meters from the baked outcrop, respectively) give the characteristic 2.37 Ga steep paleomagnetic direction. Petrophysical data (Fig. 12c) also shows that the NE-trending dyke (P27m) and baked samples have consistently higher magnetization values than the E-W dyke (BU) and unbaked samples (P27m unbaked). Both paleomagnetic and petrophysical data lend support for the primary remanence of the shallow NE direction observed in Cuddapah dykes.

5.5. Ground Magnetic Results

The negative linear magnetic anomalies associated with the dykes and their intersection are clearly distinguishable from the background field of ~41,500 nT (Fig. 5b). The narrower (~60m wide) TN dyke produces a negative anomaly with amplitude of about 300 nT. The anomaly ends at the intersection with the 110m wide TP dyke. The magnetization of TP is significantly smaller than TN, so the amplitude of the associated magnetic anomaly is also smaller. The amplitudes range between 0 and -150 nT, with an anomalous high gradient near the northern extent of TP. The low amplitudes characterize the area of intersection. The magnetic anomalies of TP are non-segmented (trend=330°) whereas the anomalies of TN are cut by TP into two parts with slightly different strikes (Fig. 5b). The western anomaly has a strike of ~085° while the easternmost section has a strike of ~075°. The gap in the otherwise negative linear anomaly as well as the lateral shift (tens of meters) associated with TN shows that the NNW-trending TP dyke is younger than the ENE-trending TN dyke. The ENE trending dyke (TN) reveals a steep reversed paleomagnetic direction (D=116.4°, I=-76.7°, α_{95}=13.7°, N=8) typical of the 2.37 Ga dykes (Table 1), while the NNW trending dyke (TP) shows a paleomagnetic direction (D=230.3°, I=-57.0°, α_{95}=11.9°, N=6) similar to the 2.21 Ga dykes (Table 2). The TP dyke also seems to be the same Great dyke of Closepet sampled by Kumar et al. (2012b) that gave two whole rock-mineral Sm-Nd ages of 2173 ± 43 Ma and 2190 ± 51 Ma and a very similar paleomagnetic direction.

6. Discussion

6.1. 2.37 Ga dykes

At least three large continental landmasses have been proposed for the Proterozoic: Kenorland (Neoarchean), Columbia (Paleo-Mesoproterozoic) and Rodinia (Neoproterozoic). Pesonen (2003) used existing paleomagnetic data at 2.45 Ga and interpreted a tentative connection between Baltica, Laurentia, Australia, and the Kalahari craton. The presence of mafic dykes and rift basins on several continents from 2.45-2.10 Ga may reflect a period of protracted continental breakup. The robust pole from the Dharwar craton at 2.37 Ga can be combined with other well dated poles from other continents in order to evaluate the paleogeography during this time interval (Fig.13; Table 6). Several poles are available for comparison with the Dharwar around 2.4 Ga (±50 Ma), including the Karelian dykes from Baltica (Mertanen et al. 1999; Salminen et al. 2013), the Matachewan dykes from the Superior craton of Laurentia (Evans and Halls 2010), and the Widgiemooltha dykes of the Yilgarn craton in northern Australia (Evans 1968; Smirnov et al. 2013).

The Widgiemooltha dyke swarm has an emplacement age of 2418 ± 3 Ma (Nemchin and Pidgeon 1998) and trends E-W. The dykes are tholeiitic and show some chemical similarities to the Dharwar dykes. Smirnov et al. (2013) reported new paleomagnetic results for the swarm using modern demagnetization techniques, and found that the datum were in good agreement with the previous study (Evans 1968). The addition of baked contacts tests now confirms the primary nature of this magnetization (Smirnov et al. 2013). Halls et al. (2007) proposed a potential link between the Yilgarn and Dharwar cratons based on the patterns of dyke swarms, and suggested that both may be the product of a single plume. Our reconstruction places the two cratons at high latitudes with about 25° of separation. The continents can be moved longitudinally so that a parallel alignment of the two swarms is possible; however, the Dharwar dykes were emplaced over a very short time (~5 Ma; Kumar et al. 2012a) and the error in ages leaves a significant gap (31 Ma minimum) between the two swarms, making it unlikely they evolved from the same plume.

The NW-SE and E-W trending Karelian dykes located in the Fennoscandian shield (Baltica) have a wide geographic extent and consist mainly of unaltered gabbronorites (Mertanen et al. 1999). A U-Pb baddeleyite age of 2339 ± 18 Ma (Dyke AD13; Salminen et al. 2013) and a Sm-Nd age of 2407 ± 35 Ma have been reported for the dykes (Dyke WD; Salminen et al. 2013; Vuollo and Huhma 2005). A recent baked contact test (Dyke WD; Salminen et al. 2013), as well as evidence for regional reheating and remagnetization of the Archean basement at ca. 2.44 Ga (Mertanen et al. 1999) lend support for a primary magnetization. The 2473–2446Ma Matachewan dykes of the Superior craton trend mainly N to NW and define a fanning angle that widens to the north (Fahrig, 1987; Halls and Bates, 1990; Heaman, 1997; Bates and Halls 1990). A primary magnetization is supported by positive baked contact tests (Schutts and Dunlop 1981; Buchan et al. 1989). New paleomagnetic (VGP) data from the Karelian Province allows us to position Baltica at either moderate (Dyke WD+Baked; 2407 ± 35 Ma) or shallow (Dyke AD13; 2339 ± 18 Ma; Salminen et al. 2013) latitudes. Each of the cratons can be positioned in the opposite hemisphere due to the ambiguity in relative polarity. Our reconstruction places the Superior craton and Baltica within about 10° latitude from each other, supporting a loose fit at 2.4 Ga. The Matachewan and Karelian dykes are sub-parallel in this configuration, providing some additional evidence for coeval emplacement. Heaman (1997) attributed the parallel trend of the dykes to a mantle plume at 2.45 Ga that may have marked the onset of rifting from the Kenorland assembly. Paleoproterozoic reconstructions are difficult due to the sparse paleomagnetic database at this time, so the addition of well-dated and precise poles like the Dharwar will help determine potential intracratonic relationships during this enigmatic period.

6.2. 2.21-2.18 dykes

Magmatism within the Dharwar craton at ~2.2 Ga may represent a widespread thermal event (French and Heaman 2010). An alternative model to the unified Kenorland assembly is the supercraton solution (Bleeker 2003). Instead of a unified supercontinent, the model employs several supercratons as the precursors to the present cratonic nuclei (Bleeker 2003). A robust paleomagnetic pole at ~2.2 Ga for the Dharwar craton may help uncover the geometries of hypothesized supercratons such as Sclavia (Dharwar-Slave connection; French and Heaman 2010). Kumar et al. (2012b) reject a possible Dharwar-Slave connection at ~2.2 Ga based on their preliminary paleomagnetic results and argue that the dissimilar Archean geology present on each craton indicates that the two evolved as separate entities and not as one coherent block.

We also sampled ~2.2 Ga dykes dated by French et al. (2004) from the NE Dharwar craton (E-W trending dolerite dyke; 2180 Ma; U-Pb baddeleyite and zircon) within the Mahbubnagar swarm (Ernst and Srivastava 2008). Our ~2.2 Ga directions differ slightly from those of Kumar et al. (2012b), with different declinations and shallower inclinations. The positive baked contact test from the Mahbubnagar dyke (Fig. 9b; this study) confirms the primary nature of this direction. Six of the dykes sampled in this study are in agreement with the directions reported by Kumar et al. (2012b); however, the primary remanence of the 2.21 Ga suite of dykes remains unconfirmed. Due to the geographic overlapping of the 2.21 and 2.18 Ga dykes, the rate of plate movement over the hypothesized plume is irresolvable; however, it is possible that the difference in paleomagnetic directions between 2.21 and 2.18 Ga (Fig.14) is due to the rotation of the Dharwar craton during this interval.

Paleomagnetic poles for the 2.23 Ga Malley dykes and 2.2 Ga Senneterre dykes are used in conjunction with both the 2.21 Ga (combined) and 2.18 Ga paleomagnetic poles from the Dharwar craton to construct a paleogeographic map at ~2.2 Ga (Fig. 14; Table 7). The NE trending Senneterre dykes of the Superior craton have a U-Pb age of 2214.3 ± 12.4 Ma (baddeleyite; Buchan et al. 1993). The Senneterre remanence is considered primary due to the secular variation observed between dykes as well as a baked contact test for the coeval Nipissing sills (Buchan 1991; Buchan et al. 1993). The NE-trending Malley dyke swarm of the Slave craton has a precise U-Pb age of 2231 ± 2 Ma (baddeleyite; Buchan et al. 2012) and extends from the central Slave craton to near the Kilohigok basin. A primary remanence has not yet been confirmed; however, a positive baked contact test at the intersection between the Malley and younger Lac de Gras dyke (2.03 Ga) and no evidence for regional overprinting lends support for a primary direction (Buchan et al. 2012).

Our reconstruction at ~2.2 Ga positions the Dharwar craton at intermediate latitudes. A north polar projection was used in an attempt to correlate the N-S trending Dharwar dykes with the NE trending dykes in the Slave craton to evaluate the possibility of the supercraton Sclavia that rifted during this interval. French and Heaman (2010) hypothesized that the present day western margin of the Dharwar craton may have been connected to the western margin of the Slave craton based on the pattern of similarly aged radiating dyke swarms. To test this configuration, we plotted the two cratons at their respective latitudes and moved them longitudinally in position for a best fit scenario. Preliminary paleomagnetic data from ~2.2 Ga

Dharwar dykes leaves about of 15° of separation between the two cratons (Figure 14). It is possible that the dyke swarms may have been coeval; however, the combined paleomagnetic pole reported here does not confirm a direct link between the two western craton boundaries.

6.3. 1.88 dykes

Twenty nine dykes from the present study, combined with the Cuddapah Traps volcanics (Clark 1982), Bastar dykes (Meert et al. 2011), Dharwar and Cuddapah dykes (Hargraves and Bhalla 1983; Kumar and Bhalla 1983; Bhalla et al. 1980; Radhakrishna et al. 2013b), and Cuddapah basin sediments (Prasad et al. 1984) provide a robust paleomagnetic pole for the Dharwar craton at ~1.9 Ga. The dual polarity magnetization present in both Bastar and Dharwar dykes as well as a positive baked contact test (this study) support a primary magnetization. Well constrained U-Pb ages from the Pullivendla sill (French et al. 2008), Cuddapah basin sediments, and a NW-SE Kunigal dyke (site 19; this study) provide age constraints for this remanence and support a connection between the Dharwar, Singhbhum, and Bastar cratons at ~1.9 Ga.

The 1.88 Ga Bastar-Cuddapah LIP event identified by French et al. (2008) is confirmed here by the presence of a large (~85,000 km^2) radiating dyke swarm within the Dharwar and Bastar cratons. Dykes to the north trend mainly NW-SE to almost N-S. The Pullivendla sill, located in the southwestern portion of the Cuddapah basin, trends roughly 290°, while dykes located south of the basin have an E-W trend. A fanning angle of 65° defines the radiating swarm, with a focal point located east of the Cuddapah basin (Fig. 3). Extension from the Godavari rift may have rotated the northern dykes counterclockwise from their original trend; however, these dykes trend mostly NW-SE, so a restorative rotation would place the dykes in a more N-S orientation, providing an even larger fan angle. The focal point of the swarm may denote the position of a 1.88 Ga mantle plume, and the NW trending positive gravity anomaly (interpreted as a mafic lensoid body) beneath the southwestern section of the Cuddapah basin could be linked to the associated plume magmatism. The Gulcheru Formation (lowest stratigraphic member) of the Cuddapah basin has a paleomagnetic direction equivalent to the ~1.9 Ga Dharwar pole, indicating that extension began in the basin at least before 1.9 Ga. A northwest trending Fe-rich tholeiite dyke with a U-Pb age of 1832 ± 72 Ma (zircon; Lanyon et al. 1993) is also present within the Vestfold Hills, East Antarctica. If we align the eastern border of the Dharwar craton against the Vestfold Hills, the dykes have a radiating pattern. Currently there is no paleomagnetic datum from the Vestfold Hills dykes, and most reconstructions place the collision between the Dharwar and East Antarctic blocks at 1 Ga during Rodinia assembly (Li et al 2008; Zhao et al. 2002), so a possible connection between the two cratons at this time is speculative.

A number of well constrained paleomagnetic poles are available at 1.88 Ga (Table 8), and allow us to test one of the possible configurations of the supercontinent Columbia (Zhao et al. 2004). Our paleomagnetically based reconstruction at 1.88 Ga is shown in Figure 15a. To test the Columbia model, continents were plotted at their respective latitudes from the paleomagnetic data (Table 8) and were moved longitudinally in position for a best fit with the Columbia configuration (Zhao et al. 2004). Poles from individual continents were selected based on the reliability of the paleomagnetic and geochronologic data, and span no more than 60 Ma apart.

Our placement of Baltica comes from the thorough Paleoproterozoic compilation of Pesonen et al. (2003), who presented a mean paleomagnetic pole for Baltica at 1.87-1.89 Ga (mean of the Vittangi, Kiuruvesi, Pohjanmaa, and Jalokoski gabbros and diorites). The paleomagnetic pole selected for Siberia comes from the 1878 ± 4 Ma Akitkan group in southern Siberia (Didenko et al. 2009). A positive fold test and intraformational conglomerate test support a primary remanence for the pole. The tentative 1.83 Ga paleomagnetic pole from the Plum Tree Volcanics of Northern Australia (Idnurm and Giddings 1988; Idnurm 2004) is used in our reconstruction. The pole may be representative of western and southern Australia as well if the arguments by Korsch et al. (2011) are correct. The Zimbabwe craton is host to the Mashonaland sills (Söderlund et al. 2010) in the northeastern part of the craton. Here we use the recalculated paleopole (Letts et al. 2011) from Evans et al. (2002) that combines dual polarity results from McElhinny and Opdyke (1964) with results from Bates and Jones (1996). The paleomagnetic pole selected for the Superior craton is the recalculated 1.87 Ga Molson-B+C2 pole (Halls and Heaman 2000; Zhai et al. 1994; Evans and Halls 2010), and the pole used for the Slave craton comes from the 1.88 Ga Ghost dykes (Buchan p.comm.). Paleomagnetic poles from the Kaapvaal craton come from the 1.87-1.88 Ga Black Hills and post-Waterberg dykes in northern South Africa (Hanson et al. 2004; de Kock 2007; Lubina et al. 2010). The Kaapvaal and Zimbabwe cratons collided during the interval from 1.90 to 2.06 Ga (Lubina et al 2010), and our reconstruction places the two in close proximity at 1.9 Ga.

Similarities between the paleomagnetic-based reconstruction and that of Zhao et al. (2004) include the relationship between Baltica and the Superior craton (Figs. 15a and b). Our reconstruction places Baltica at equatorial to mid-latitudes and Superior at mid-high latitudes. The main difference between the two models is the equatorial position of India at 1.9 Ga (Figure 15a). The archetypal Columbia model places India at higher latitudes adjacent to the North China craton along with the Australian and South African nuclei. Here the Australian and South African blocks occupy mid-latitudinal positions, however; the proposed relationship between the blocks is consistent with the geologic model (Figs. 15a and b; Zhao et al. 2004). In the archetypal Columbia fit, Siberia is located just north of the Laurentian margin at high latitudes.

Paleomagnetic data from Didenko et al. (2009) used in our reconstruction places Siberia at more equatorial latitudes, and is in sharp contrast to the continental relationships proposed by Zhao et al. (2004). Hoffman (1988; 1989ab; 1997) proposed a close relationship between Laurentia, Baltica, and Siberia within the Columbia (Nuna) supercontinent based on the similarities between the Archean Nain and Karelia cratons, the Ketilidian and Svecofennian orogens, the Labrador and Gothian Orogens, and extensions of the Slave-Churchill collision zone (Thelon Orogen) across the Arctic. Our reconstruction shows a 70° latitudinal spread of the three continents, and does not support a close relationship at 1.9 Ga. Hou et al. (2008) proposed a configuration for the supercontinent at 1.85 Ga based on the alignment of orogenic zones and patterns of radiating dyke swarms (Fig. 15c). Key differences between our reconstruction and the former include the relative positions of India and Siberia within the supercontinent. Hou et al. (2008) place Siberia at intermediate latitudes 20° north of Baltica, while our reconstruction positions both Siberia and Baltica near the equator. Peninsular India is positioned at mid-latitudes and linked with the Canadian Shield in the 1.85 Ga reconstruction; however, our paleomagnetic pole places India at the equator with about 20° of latitudinal separation from the Superior craton (Figs. 15a and c). Pisarevsky et al. (2013b) suggest a long-term India-Baltica fit between the Dharwar and Sarmatia cratons using the Lakhna dykes pole and ophiolites (1850-1330 Ma) in the Eastern Ghats. They propose a protocraton consisting of the western margin of the Dharwar against the southwestern accretionary margin of Baltica. Our 1.88 Ga reconstruction places these two in close latitudinal position; however, the orientations of each craton do not allow this type of fit, so the model faces problems here.

The addition of well-constrained paleomagnetic poles from 2.37-1.88 Ga allows us to construct an APWP for the Dharwar craton during this interval (Fig. 16). Paleolatitudes were calculated from each direction using central site locations in the Dharwar craton and using only north poles. At 2.37 Ga, a steep inclination corresponds to a paleolatitude of 74°N, at 2.21 and 2.18 Ga intermediate inclinations correspond to paleolatitudes of 47.7°N and 37°N, and at 1.88 Ga a shallow inclination corresponds to a paleolatitude of 2.1°N. True plate velocity is calculated from the combination of latitude, longitude, and rotation; however, longitude is unconstrained here so we calculate the minimum rates for latitude and rotation along one line of longitude. An average latitudinal rate is about 2 cm/yr and average rotational rate is about 5 cm/yr during the Paleoproterozoic.

6.4 Cuddapah dykes

The mean paleomagnetic direction from the Cuddapah dykes is similar to the direction reported for the Karimnagar dykes (Rao et al. 1990; Kumar et al. 2012a; Table 4). The unusually large within-site scatter of the Karimnagar dykes (Rao et al. 1990), as well as similar directions in remote host rocks (comprised of charnokites; Bhimasankaram 1964) have led to a debate regarding the primary nature of this direction (e.g. Halls et al. 2007; Kumar et al. 2012a). Kumar et al. (2012a) classified this shallow NE direction as a secondary magnetization by comparing Karimnagar dykes to the Dharwar giant dyke swarm using precise U-Pb dating, paleomagnetism, and geochemical analysis. Kumar et al. (2012b) also report a similar secondary overprint (Component S; Table 4) in multiple sites along the Great dyke of Closepet (parallels the eastern margin of Closepet granite for ~350 km); however, the origin and age of this direction is still undetermined.

Our positive baked contact test (crosscutting dykes, site P27m; Fig.12) is located in the same area as the baked contact test conducted by Kumar and Bhalla (1983). They reported a positive test for the Great dyke of Penukonda and concluded that this dyke crosscuts the NE trending dyke; however, the cross-cutting relationship of these dykes is not clear from recent field observations (This study). Our new baked contact test combined with the petrophysical data supports a primary remanence in the NE trending dyke, and allows us to reclassify the crosscutting relationship (E-W trending Great dyke of Penukonda is older than the NE-trending dyke). The low loss on ignition values also indicates negligible alteration in the NE dykes (P27 and P29; Piispa et al. 2011). Furthermore, the geochemical signature of the NE-trending dykes (P27 and P29) is distinct from both the Bengaluru dyke swarm as well as the Karimnagar dykes (Piispa et al. 2011; Kumar et al. 2012a) suggesting that these dykes represent a separate swarm located around the Cuddapah basin. Additional geochemical analysis of the Cuddapah dykes will help confirm this relationship.

The precise age of the Great dyke of Penukonda (2365.9±2.6 Ma; French and Heaman 2010), combined with the positive baked contact test and the presence of the same shallow overprint observed in 2.21 Ga dykes, provides an upper estimate for the age of the shallow NE direction. The similarity between the secondary component observed in the Cuddapah dykes (see P27i and P29i in Piispa et al. 2011) and the typical ~1.9 Ga direction provides a minimum age constraint. Two NW trending dykes (BS and 597; Table 3) with the typical ~1.9 direction located near the cross-cutting Bukkapatnam dykes may be responsible for this chemical remanent magnetization. The shallow NE direction is similar to other units within Peninsular India, including the Gwalior traps from the Bundelkhand craton (Pradhan et al. 2010), the secondary component observed in the ~2500-2100 Ma Charnokites of the Southern Granulite Terrane (Mondal et al. 2009), as well as Bundelkhand, Bastar, and Dharwar mafic dykes (Radhakrishna et al. 2013a,b). The EDC granites and gneisses have Rb–Sr whole rocks ages between ~2545 Ma and 2128 Ma (Pandey et al., 1997), and Halls et al. (2007) proposed that a regional heating event at ~2.1 Ga was responsible for the observed Karimnagar overprint. Deformation and ultra-high temperature metamorphism have also been observed in the CITZ around this time (2040±17 Ma; Mohanty, 2010, 2012). This large scale event in Peninsular India at 2.1 Ga and the associated Cuddapah dykes may indicate the arrival of a mantle plume responsible for the formation of the Cuddapah basin.

7. Conclusions

Paleomagnetic evidence for multiple episodes of continental assembly and breakup in earth's history support an inherent cyclicity to the supercontinent cycle. While there is no current consensus on the exact make-up and geometry of the supercontinent Columbia, the addition of new paleomagnetic poles and precise U-Pb ages will help clarify the configuration of some of the Earth's earliest landmasses. Our reconstruction at 1.88 Ga demonstrates that the history of continental assembly and dispersal is complex and that the traditional geologic models need some reevaluation in spite of new robust paleomagnetic data. Below we list the main conclusions of this study.

1. Paleomagnetism of 14 dykes from the present study strengthens the combined dataset for the Dharwar craton at 2.37 Ga. The dykes are part of the E-W trending Dharwar giant dyke swarm (Halls et al. 2007; Kumar et al. 2012a), and our baked contact test now confirms the primary nature of this magnetization. While the majority of dykes trend E-W, we cannot reject the hypothesis of a radiating swarm from Godavari-related tectonics. The combined paleomagnetic pole places India at polar latitudes during the early Paleoproterozoic, and represents one of the most robust paleomagnetic poles for this era.

2. We present two paleomagnetic poles for the Dharwar craton at ~2.2 Ga representing the separate magmatic suites identified by French and Heaman (2010) at 2.21 and 2.18 Ga. Recent paleomagnetic results from Kumar et al. (2012b) are most likely from the 2.21 suite of dykes (Srivastava et al. 2011); however, a primary remanence is still unconfirmed. We report paleomagnetic results from the well dated 2.18 Ga Mahbubnagar swarm (French et al. 2004; Ernst and Srivastava 2008) and provide a positive baked contact test for the dykes. Using existing well dated paleomagnetic poles from the Slave and Superior cratons we provide a reconstruction at ~2.2 Ga, and show a 30° latitudinal separation between the three blocks.

3. We confirm the Southern Bastar-Cuddapah LIP event (French et al. 2008; Ernst and Srivastava 2008) through the presence of a large (~85,000 km^2) radiating dyke swarm within the Dharwar craton at 1.88 Ga. The swarm has a fanning angle of 65°, defined by NNW-SSE trending dykes located north of the Cuddapah basin, the NW-SE (290°) trending Pullivendla mafic sill, and the E-W trending dykes located west of the basin. The dykes converge at a focal point located east of the Cuddapah basin that may mark the position of an ancient plume. Extension within the Papaghani sub-basin most likely initiated as a result of this plume-related magmatism. Further evidence comes from a gravity imaged mafic lensoid body beneath the southwestern Cuddapah basin (Bhattacharji and Singh 1984) and the associated intrusive Cuddapah volcanics.

4. The paleomagnetic dataset reported here yields a precise paleomagnetic pole for the Dharwar craton (and possibly greater India) at ~1.9 Ga. The well-constrained ages from the Pullivendla mafic sill, Bastar dykes, and a Kunigal dyke (this study) provide a robust geochronologic age for the pole and support a connection between the Bastar, Dharwar, and Singhbhum cratons at this time. Using well-dated poles from other continents at 1.88 Ga, we tested a possible configuration for the Columbia supercontinent. Well-accepted models for the supercontinent propose continental breakup at 2.2-2.0 and assembly at 1.9-1.7 Ga. The paleomagnetic-based reconstruction at 1.88 Ga indicates that if the Columbia supercontinent was assembled at this time, the proposed models need modification (Zhao et al. 2002, 2004; Hou et al. 2008; Rogers and Santosh 2002; Hoffman 1988, 1989ab, 1997), and many of the linked geologic similarities are inconsistent with the most reliable poles.

5. We propose that the large scale regional heating event observed in the Dharwar craton at ~2.1 Ga and the Cuddapah dyke swarm (with shallow NE paleomagnetic direction) are related and that these events reflect the emplacement of a mantle plume responsible for the initial formation of the Cuddapah basin.

Acknowledgements

This work was supported by a grant from the US National Science Foundation to J.G. Meert (EAR09-10888). We thank Candler C. Turner, M. Lingadevaru, Shashi Kala Chandrappa, and Anantha Murthy for their assistance with field work and Carlos Ortega for assistance in geochronology.

References

Anand, M., Gibson, S. A., Subbarao, K. V., Kelley, S. P.&Dickin, A. P. 2003. Early Proterozoic melt generation processes beneath the intra-cratonic Cuddapah basin, Southern India. Journal of Petrology, 44, 2139–2171.

Balakrishnan, S., Hanson, G.N., Rajamani, V., 1990. Pb and Nd isotope constraints on the origin of high Mg and tholeiite amphibolites, Kolar schist belt, southern India. Contribution Minerals and Petroleum 107, 272–292.

Bates, M.P., and Halls, H.C. 1990. Regional variation in paleomagnetic polarity of the Matachewan dyke swarm related to the Kapuskasing structural zone, Ontario. Canadian Journal of Earth Sciences, 27: 200–211.

Bates, M. P. & Jones, D. L. 1996. A palaeomagnetic investigation of the Mashonaland dolerites, north-east Zimbabwe. Geophysical Journal of International,126, 513–524.

Benton, M.J. Vertebrate Palaeontology. Third edition (Oxford 2005), 25.

Biswas, S. K., 2003. Regional tectonic framework of the Pranhita–Godavari basin, India. Journal of Asian Earth Sciences, 21(6), 543-551.

Bhalla, M.S., Hansraj, A., Prasada Rao, N.T.V., 1980. Paleomagnetic studies of Bangarpet and Sargur dykes of Precambrian age from Karnataka, India. Geoviews 8, 181–189.

Bhandari, A., Pant, N.C., Bhowmik, S.K., Goswami, S., 2010. ~1.6 Ga ultrahightemperature granulite metamorphism in the Central Indian Tectonic Zone: insights from metamorphic reaction history, geothermobarometry and monazite chemical ages. Geological Journal 45, 1–19.

Bhaskar Rao, Y.J., Pantulu, G.V.C., Damodara Reddy, V., Gopalan, V., 1995. Time of early sedimentation and volcanismin the Proterozoic Cuddapah Basin, South India: evidence from the Rb–Sr age of Pulivendla mafic sill. Devaraju, T.C. (Ed.), Mafic Dyke Swarms of Peninsular India, Mem. Geol. Soc. India, no.33, pp.329-338.

Bhattacharji, S. & Singh, R. N. 1984. Thermomechanical structure of the southern part of the Indian Shield and its relevance to Precambrian basin evolution. Tectonophysics, 105, 103–120. Bhimasankaram, V. L. S. (1964), A preliminary investigation on the paleomagnetic directions of the charnockites of Andhra Pradesh, Curr. Sci., 33, 465–466.

Bhowmik, S.K.,Wilde, S.A., Bhandari, A., 2011. Zircon U–Pb/Lu–Hf and Monazite chemical dating of the Tirodi biotite gneiss: implication for latest Palaeoproterozoic to Early Mesoproterozoic orogenesis in the Central Indian Tectonic Zone. Geological Journal 46, 574–596.

Bhowmik, S. K., Wilde, S. A., Bhandari, A., Pal, T., and Pant, N. C., 2012. Growth of the Greater Indian Landmass and its assembly in Rodinia: Geochronological evidence from the Central Indian Tectonic Zone. Gondwana Research 22, no. 1, p. 54-72.

Bispo-Santos, F., D'Agrella-Filho, M. S., Pacca, I. I., Janikian, L., Trindade, R. I., Elming, S. A., Silva, J.A., Barros, M.A.S., Pinho, F. E. C., 2008. Columbia revisited: paleomagnetic results from the 1790Ma colider volcanics (SW Amazonian Craton, Brazil). Precambrian Research, 164(1), 40-49.

Bleeker, W. 2003. The Archean record: A puzzle in ca. 35 pieces. Lithos, 71(2–4): 99–134.

Buchan, K. L., Neilson, D., and Hale, C. J., 1989. Relative ages of Matachewan dykes and Otto stock from paleomagnetism [abstract]. Canadian Geophysical Union, Program and Abstracts 16: 75.

Buchan, K.L. 1991. Baked contact test demonstrates primary nature of dominant (Nl) magnetisation of Nipissing intrusions in Southern Province, Canadian Shield. Earth and Planetary Science Letters,105: 492 -499.

Buchan, K.L., Mortensen, J.K., and Card, K.D. 1993. Northeast trending Early Proterozoic dykes of southern Superior Province: multiple episodes of emplacement recognized from integrated paleomagnetism and U–Pb geochronology. Canadian Journal of Earth Sciences, 30(6): 1286–1296.

Buchan, K.L., Mertanen, S., Park, R.G., Pesonen, L.J., Elming, S.-Å., Abrahamsen, N., and Bylund, G. 2000. Comparing the drift of Laurentia and Baltica in the Proterozoic: the importance of key palaeomagnetic poles. Tectonophysics, 319(3): 167–198.

Buchan, K.L., LeCheminant, A.N., and van Breemen, O. 2009. Paleomagnetism and U–Pb geochronology of the Lac de Gras diabase dyke swarm, Slave Province, Canada: implications for relative drift of Slave and Superior provinces in the Paleoproterozoic. Canadian Journal of Earth Sciences, 46(5): 361–379.

Buchan, K.L., LeCheminant, A.N., Breemen, O., 2012. Malley diabase dykes of the slave craton, Canadian Shield: U-Pb age, paleomagnetism, and implications for continental reconstructions in the early Paleoproterozoic. Can. J., Earth Sci. 49, 435-454.

Chadima, M., and Jelinek, V., 2012. Cureval 8 [computer software]. Brno, Czech Republic. Retrieved from http://www.agico.com/software/winsoft/cureval/download.php

Chadwick, B., Vasudev, V.N., Hegde, G.V., 2000. The Dharwar Craton, southern India, interpreted as the result of late Archean oblique convergence. Precambrian Research 99, 91–111.

Chardon, D., Peucat, J.-J., Jayananda, M., Choukroune, P., Fanning, C.M., 2002. Archaean granite–greenstone tectonics at Kolar (south India): interplay of diapirism and bulk homogenous contraction during juvenile magmatic accretion. Tectonics 21, 1016,

Chaudhuri, A.K., Deb, G., 2004. Proterozoic rifting in the Pranhita–Godavari valley: implication on India–Antarctica linkage. Gondwana Research 7, 301–312.

Clark, D.A., 1982. Preliminary paleomagnetic results from the Cuddapah traps of Andhra Pradesh, Monograph-2, On Evolution of the intracratonic Cuddapah Basin. HPG, Hyderabad, India, pp. 47–51.

Condie, K.C., 2002a. Continental growth during a 1.9-Ga superplume event. J. Geodyn. 34, 249–264.

Condie, K.C., 2002b. Breakup of a Paleopreoterozoic supercontinent. Gondwana Research 5, 41–43.

Crawford, A.R., Compston, W., 1969. The age of the Vindhyan System of Peninsular India. Quaternary Journal of Geological Society of London 125, 351–371.

Dash, J.K., Pradhan, S.K., Bhutani, R., Balakrishnan, S., Chandrasekaran, G and Basavaiah, N. 2013. Paleomagnetism of ca. 2.3 Ga mafic dyke swarms in the northeastern Southern Granulite Terrain, India: Constraints on the position and extent of Dharwar craton in the Paleoproterozoic. Precambrian Research.

Dawson, E.M., Hargraves, R.B., 1994. Paleomagnetism of Precambrian swarms in the Harohalli area, south of Bangalore, India. Precambrian Res. 69, 157–167.

de Kock, M.O. 2007. Paleomagnetism of selected Neoarchean–Paleoproterozoic cover sequences on the Kaapvaal craton and implications for Vaalbara. Unpublished Ph.D. Thesis. University of Johannesburg, Johannesburg 276 pp.

Didenko, A.N., Vodovozov, V.Y., Pisarevsky, S.A., Gladkochub, D.P., Ladkochub, D., Donskaya, T.V., Mazukabzov, A.M., Mazukabzov, A., Stanevich, A.M., Stanevich, A., Bibikova, E.V., Bibikova, Y., Kirnozova, T.I., 2009. Palaeomagnetism and U–Pb dates of the Palaeoproterozoic Akitkan Group (south Siberia) and implications for pre-Neoproterozoic tectonics. In: Reddy, S.M., Mazumder, R., Evans, D.A., David, A.D., Collins, A.S. (Eds.), Palaeoproterozoic Supercontinents and Global Evolution, 323. Geological Society Special Publication, pp. 145–163.

Domeier, M., Van der Voo, R., Torsvik, T.H. 2012. Review Article: Paleomagnetism and Pangea: The Road to reconciliation. Tectonophysics 514-517, 14-43.

Elming, S.-Å., Mattsson, H., 2001. Post Jotnian basic intrusion in the Fennoscandian Shield, and the breakup of Baltcia from Laurentia: a palaeomagnetic and AMS study. Precambrian Research 108, 215–236.

Ernst, R.E., Srivastava, R.K., 2008. India's place in the Proterozoic world: constraints from the large igneous provinces (LIP) record. In: Srivastava, R.K., Sivaji, Ch., Chalapathi Rao, N.V. (Eds.), Indian Dykes: Geochemistry, Geophysics, and Geochronology. Narosa Publishing House Pvt. Ltd, New Delhi, India, pp. 41–56.

Ernst, R.E., Srivastava, R.K., Bleeker, W., Hamilton, M., 2010. Precambrian Large Igneous Provinces (LIPs) and their dyke swarms: new insights from high-precision geochronology integrated with paleomagnetism and geochemistry. Precambrian Research 183, vii–xi.

Evans, D. A. D., Beukes, N. J. & Kirschvink, J. L., 2002. Paleomagnetism of a lateritic paleoweathering horizon and overlying Paleoproterozoic red beds from South Africa: implications for the Kaapvaal apparent polar wander path and a confirmation of atmospheric oxygen enrichment. Journal of Geophysical Research 107.

Evans, D. A. D., and Halls, H. C. 2010. Restoring Proterozoic deformation within the Superior craton. Precambrian Research 183(3), 474-489.

Evans, D.A., and Mitchell, R. N., 2011. Assembly and breakup of the core of Paleoproterozoic–Mesoproterozoic supercontinent Nuna. Geology 39, p. 443-446.

Evans, M.E., 1968. Magnetization of dikes: a study of the paleomagnetism of the Widgiemooltha dike suite, Western Australia. J. Geophys. Res. 73, 32361-33270.

Everitt, C. W. F., & Clegg, J. A., 1962. A field test of palaeomagnetic stability. Geophysical Journal International, 6(3), 312-319.

Fahrig, W. F. 1987. The tectonic settings of continental mafic dyke swarms: failed arm and early passive margin. In Mafic dyke swarms. Edited by H. C. Halls and W. F. Fahng. Geological Association of Canada, Special Paper 34, pp. 33 1-348.

Fisher, R.A., 1953. Dispersion on a sphere. Proceedings Royal Society A, 217, pp. 295–305.

French, J. E., Heaman, L. M., Chacko, T. and Rivard, B. (2004) Global mafic magmatism and continental breakup at 2.2 Ga: evidence from the Dharwar craton, India. Geol. Soc. America Abstracts with Program, v.36 (5), p.340.

French, J.E., Heaman, L.M., Chacko, T., Srivastava, R.K., 2008. 1891–1883 a southern Bastar craton-Cuddapah mafic igneous events, India: a newly recognized large igneous province. Precambrian Research 160, 308–322.

French, J.E. and Heaman, L.M., 2010. Precise U-Pb dating of Paleoprotoerozoic mafic dyke swarms of the Dharwar craton, India: Implications for the existence of the Neoarchean supercraton Sclavia. Precambrian Research 183, 416-441.

Friend, C.R.L., Nutman, A.P., 1991. SHRIMP U–Pb geochronology of the Closepet granite and Peninsula gneisses, Karnataka, South India. Journal of Geological Society India 32, 357–368.

Halls, H.C., Heaman, L.M., 2000. The paleomagnetic significance of new U–Pb age data from the Molson dyke swarm, Cauchon Lake area, Manitoba. Canadian Journal of Earth Sciences 37, 957–966.

Halls, H.C., Kumar, A., Srinivasan, R., Hamilton, M.A., 2007. Paleomagnetism and U–Pb geochronology of easterly trending dykes in the Dharwar craton, India: feldspar clouding, radiating dyke swarms and the position of India at 2.37 Ga. Precambrian Research 155, 47–68.

Hanson, R.E., Gose, W.A., Crowley, J.L., Ramezani, J., Bowring, S.A., Bullen, D.S., Hall, R.P., Pancake, J.A., 2004. Paleoproterozoic intraplate magmatism and basin development on the Kaapvaal Craton: Age, paleomagnetism and geochemistry of ~1.93 to ~1.87 Ga post-Waterberg dolerites. S. Afr. J. Geol. 107, 233–254.

Hargraves, H. B. and Bhalla, M.S. (1983) Precambrian paleomagnetism in India through 1982: a review. In: S. M. Naqvi and J. J. W. Rogers (Eds.), Precambrian of South India. Geol. Soc. India Mem. 4, 491-524.

Hasnain, J., Qureshy, M.N., 1971. Paleomagnetism and geochemistry of some dykes in Mysore State, India. J. Geophys. Res. 76, 4786–4795.

Heaman, L.M., 1997. Global mafic magmatism at 2.45 Ga: remnants of an ancient large igneous province? Geology 25, 299–302.

Hoffman, P.F., 1988. United Plates of America, the birth of a craton; Early Proterozoic assembly and growth of Laurentia. Ann. Rev. Earth Planet. Sci.16, 543–603.

Hoffman, P.F., 1989a. Speculations on Laurentia's first gigayear (2.0-1.0 Ga). Geology 17, 135-138.

Hoffman, P.F., 1989b. Precambrian geology and tectonic history of North America in: The Geology of North America: An Overview (eds. A.W. Bally and A.R. Palmer), Geological Society of America, pp.447-511.

Hoffman, P.F., 1997. Tectonic genealogy of North America. In Earth Structure. in :An Introduction to Structural Geology and Tectonics, eds. B.A. van der Pluijm and S. Marshak, New York: McGraw-Hill, 459-464.

Hou, G., Santosh, M., Qian, X., Lister, G.S., Li, J., 2008. Configuration of the Late Paleoproterozoic supercontinent Columbia: insights from the radiating mafic dyke swarms. Gondwana Research 14, 385–409.

Idnurm, M., 2004. Precambrian palaeolatitudes for Australia—an update. Report prepared for Geoscience Australia. Canberra, p. 20.

Idnurm, M., Giddings, J.W., 1988. Australian Precambrian polar wander: a review. Precambrian Research 40/41, 61–88.

Jayananda, M., Chardon, D., Peucat, J.J., Capdevila, R., 2006. 2.61 Ga potassic granites and crustal reworking in the western Dharwar craton, southern India: tectonic, geochronologic and geochemical constraints. Precambrian Research 150, 1–26.

Jayananda, M., Martin, H., Peucat, J.-J. and Mahabaleshwar, B. (1995) Late Archaean crust mantle interaction: geochemistry of LREE enriched mantle derived magmas. Example of the Closepet batholith, southern India. Contrib. Mineral. Petrol., v.119, pp.314-329.

Jayananda, M., Moyen, J.F., Martin, H., Peucat, J.J., Auvray, B., Mahabaleshwar, B., 2000. Late Archean (2550–2520 Ma) juvenile magmatism in the eastern Dharwar craton, southern India: constraints from geochronology, Nd–Sr isotopes and whole rock geochemistry. Precambrian Research 99, 225–254.

Kirschvink, J.L., 1980. The least squares line and plane and the analysis of paleomagnetic data. Geophys. J. Royal Astron. Soc. 62, 699-718.

Korsch, R.J., Kositcin, N., Champion, D.D., 2011. Australian island arcs through time: geodynamic implications for the Archean and Proterozoic. Gondwana Research 19, 716–734.

Kumar, A., Bhalla, M.S., 1983. Paleomagnetics and igneous activity of the area adjoining the southwestern margin of the Cuddapah basin, India. Geophys. J. Royal Astron. Soc., 73, 27-37.

Kumar, A., Hamilton, M.A., Halls, H., 2012a. A Paleoproterozoic giant radiating dyke swarm in the Dharwar Craton, southern India. Geochem. Geophys. Geosyst., 13, doi: 541 10. 1029/2011GC003926.

Kumar, Anil, Nagaraju, E., Besse, Jean, Rao, Y.J. Bhaskar, 2012b. New age, geochemical and paleomagnetic data on a 2.21 Ga dyke swarm from south India: Constraints on Paleoproterozoic reconstruction, Precambrian Research, Volumes 220–221, Pages 123-138.

Lanyon, R., Black, L. P., & Seitz, H. M., 1993. U-Pb zircon dating of mafic dykes and its application to the Proterozoic geological history of the Vestfold Hills, East Antarctica. Contributions to Mineralogy and Petrology 115(2), 184-203.

Letts, S., Torsvik, T. H., Webb, S. J., & Ashwal, L. D., 2011. New Palaeoproterozoic palaeomagnetic data from the Kaapvaal Craton, South Africa. Geological Society, London, Special Publications *357*(1), 9-26.

Li, Z.X., S.V. Bogdanova, Collins A.S., Davidson A., De Waele B., Ernst R.E., Fitzsimons I.C.W., Fuck R.A., Gladkochub D.P., Jacobs J., Karlstrom K.E., Lu S., Natapov L.M.,

Lubnina, N.V., Ernst, R., Klausen, M., Söderlund, U., 2010. Paleomagnetic study of

NeoArchean–Paleoproterozoic dykes in the Kaapvaal craton. Precambrian Research 183, 523–552.

McElhinny, M.W., and Opdyke, N. D., 1964. The paleomagnetism of the Precambrian dolerites of eastern Southern Rhodesia, an example of geologic correlation by rock magnetism. Journal of Geophysical Research, 69(12), 2465-2475.

McFadden, P.L., McElhinney, M.W., 1990. Classification of the reversal test in paleomagnetism. Geophysical Journal International 103, 725–729.

Meert, J.G., 2002. Paleomagnetic evidence for a Paleo-Mesoproterozoic supercontinent Columbia. Gondwana Research 5, 207–216.

Meert, J.G., 2012. What's in a name? The Columbia (Paleopangaea/Nuna) supercontinent, Gondwana Research, Volume 21, Issue 4, May 2012, Pages 987-993.

Meert, J.G. and Lieberman, B.S., 2008. The Neoproterozoic assembly of Gondwana and its relationship to the Ediacaran-Cambrian Radiation, Gondwana Research, 14, 5-21.

Meert, J.G., Pandit, M.K., Pradhan, V.R., Banks, J.C., Sirianni, R., Stroud, M., Newstead, B., Gifford, J., 2010. The Precambrian tectonic evolution of India: A 3.0 billion year odyssey, Journal of Asian Earth Sciences 39, 483-515.

Meert, J.G., Pandit, M.K., Pradhan, V.R., 2011. Preliminary report on the paleomagnetism of 1.88 Ga dykes from the Bastar and Dharwar cratons, Peninsular India. Gondwana Research, doi:10.1016/j.gr.2011.03.005.

Meert, J.G., Powell, C. McA., 2001. Assembly and breakup of Rodinia. Precambrian Research 110, 1–8.

Meert, J.G., Torsvik, T.H., 2003. The making and unmaking of a supercontinent: Rodinia revisted. Tectonophysics 375, 261–288.

Mertanen, S., Halls, H. C., Vuollo, J. I., Pesonen, L. J., & Stepanov, V. S., 1999. Paleomagnetism of 2.44 Ga mafic dykes in Russian Karelia, eastern Fennoscandian Shield—implications for continental reconstructions. Precambrian Research 98(3), 197-221.

Mohanty, S., 2010. Tectonic evolution of the Satpura Mountain Belt: A critical evaluation and implication on supercontinent assembly. Journal of Asian Earth Sciences, 39(6), 516-526.

Mohanty, S., 2012. Spatio-temporal evolution of the Satpura Mountain Belt of India: A comparison with the Capricorn Orogen of Western Australia and implication for evolution of the supercontinent Columbia. Geoscience Frontiers, 3(3), 241-267.

Mondal, S., Piper, J.D.A., Hunt, L., Bandyopadhyay, G., Basu Mallik, S., 2009. Palaeomagnetic and rock magnetic study of charnockites from Tamil Nadu, India, and the 'Ur' protocontinent in Early Palaeoproterozoic times. Journal of Asian Earth Sciences 34, 493–506.

Moyen, J.-F., Martin, H., Jayananda, M., Mahabaleswar, B., Auvray, B., 2003. From the roots to the roof of a granite: the Closepet granite, south India. J. Geol. Soc. India 62-6, 753–768.

Mueller, P.A., Kamenov, G.D., Heatherington, A.L., Richards, J., 2008. Crustal evolution in the Southern Appalachian Orogen; evidence from Hf isotopes in detrital zircons. Journal of Geology 116, 414–422.

Murty, Y.G.K., Babu Rao, V., Guptasarma, D., Rao, J.M., Rao, M.N., Bhattacharji, S., 1987. Tectonic, petrochemical and geophysical studies of mafic dyke swarms around the Proterozoic Cuddapah basin, South India. In: Halls, H.C., Fahrig, W.F. (Eds.), Mafic Dyke Swarms. Geological Association of Canada Special Paper, vol. 34, pp. 303–316.

Naganjaneyulu, K., & Santosh, M., 2010. The Central India Tectonic Zone: a geophysical perspective on continental amalgamation along a Mesoproterozoic suture. Gondwana Research 18(4), 547-564.

Nagaraja Rao, B.K., Rajurkar, S.T., Ramalingaswamy, G., Ravindra Babu, B., 1987. Stratigraphy, structure and evolution of the Cuddapah Basin. In: Purana Basins of Peninsular India (Middle to Late Proterozoic), vol. 6. Geological Society of India Memoir, pp. 33–86.

Naqvi, S.M., Divakar Rao, V., Narain, H., 1974. The protocontinental growth of the Indian shield and the antiquity of its rift valleys. Precambrian Research 1, 345–398.

Naqvi, S.M., Rogers, J.J.W., 1987. Precambrian Geology of India. Oxford University Press, Oxford, 223 pp.

Nemchin, A.A., Pidgeon, R.T., 1998. Precise conventional and SHRIMP baddeleyite age for the Binneringie dyke near Narrogin, Western Australia. Australian J. Earth Sci. 45, 673-675.

Noble, S.R., Lightfoot, P.C., 1992. U-Pb baddeleyite ages of the Kerns and Triangle Mountain intrusions, Nipissing Diabase, Ontario. Can. J. Earth Sci. 29, 1424-1429.

Nutman, A.P., Hagiya, H., Maruyama, S., 1995. SHRIMP U-Pb single zircon geochronology of a Proterozoic mafic dyke, Isukasia, Southern West Greenland. Geol. Soc. Denmark Bull. 42, 17-22.

Pandey, B.K., Gupta, J.N., Sarma, K.J., Sastry, C.A., 1997. Sm–Nd, Pb–Pb and Rb–Sr geochronology and petrogenesis of the mafic dyke swarm of Mahbubnagar, south India:

implications for Paleoproterozoic crustal evolution of the eastern Dharwar craton. Precambrian Res. 84, 181–196.

Pease, V., Pisarevsky, S.A., Thrane, K., Vernikovsky, V., 2008. Assembly, configuration, and break-up history of Rodinia: A synthesis. Precambrian Research 160, 179-210.

Pesonen, L.J., Elming, S.Å., Mertanen, S., Pisarevsky, S., D'Agrella-Filho, M.S., Meert, J.G., Schmidt, P.W., Abrahamsen, N., Bylund, G., 2003. Palaeomagnetic configuration of continents during the Proterozoic. Tectonophysics 375, 289–324.

Pesonen, L. J., Mertanen, S., & Veikkolainen, T., 2012. Paleo-Mesoproterozoic Supercontinents–A Paleomagnetic View. Geophysica 48(1-2), 5-47.

Piispa, E. J., Smirnov, A. V., Pesonen, L. J., Lingadevaru, M., Anantha Murthy, K. S., & Devaraju, T. C. (2011). An Integrated Study of Proterozoic Dykes, Dharwar Craton, Southern India. Dyke Swarms: Keys for Geodynamic Interpretation. Springer-Verlag Berlin Heidelberg 2011, chp 3, p. 33-45.

Piper, J.D.A., 2010. Protopangaea: Palaeomagnetic definition of Earth's oldest (mid-Archaean-Palaeoproterozoic) supercontinent. Journal of Geodynamics 50, 3-4, 154-165.

Pisarevsky, S. A., Sokolov, S.J., 1999. Palaeomagnetism of the Palaeoproterozoic ultramafic intrusion near Lake Konchozero, Southern Karelia, Russia. Precambrian Research 93, 201– 213.

Pisarevsky, Sergei A., Biswal, Tapas Kumar, Wang, Xuan-Ce, De Waele, Bert, Ernst, Richard, Söderlund, Ulf, Tait, Jennifer A., Ratre, Kamleshwar, Singh,Yengkhom Kesorjit, Mads Cleve, 2013a. Palaeomagnetic, geochronological and geochemical study of Mesoproterozoic Lakhna Dykes in the Bastar Craton, India: Implications for the Mesoproterozoic supercontinent. Lithos 174, 125-143.

Pisarevsky, S. A., Elming, S. Å., Pesonen, L. J., & Li, Z. X., 2013b. Mesoproterozoic paleogeography: Supercontinent and beyond. Precambrian Research.

Pradhan, V.R., Pandit, M.K., Meert, J.G., 2008. A cautionary note on the age of the paleomagnetic pole obtained from the Harohalli dyke swarms, Dharwar craton, southern India. In: Srivastava, et al. (Ed.), Indian Dykes. Narosa Publishing House, New Delhi, India, pp. 339–352.

Pradhan, V.R., Meert, J.G., Pandit, M.K., Kamenov, G., Gregory, L.C. and Malone, S.J., 2010. India's changing place in global Proterozoic reconstructions: New geochronologic constraints on key paleomagnetic poles from the Dharwar and Aravalli/Bundelkhand cratons, Journal of Geodynamics, 50, 224-242.

Pradhan, Vimal R., Meert, Joseph G., Pandit, Manoj K., Kamenov , George, Mondal, Md. Erfan Ali, 2012. Paleomagnetic and geochronological studies of the mafic dyke swarms of Bundelkhand craton, central India: Implications for the tectonic evolution and paleogeographic reconstructions, Precambrian Research, Volumes 198–199, Pages 51-76.

Prasad CVRK, Pulla Reddy V, Subba Rao KV, Radhakrishna Murthy C (1987) Palaeomagnetism and the crescent shape of the Cuddapah basin. Geol Soc India Mem 6: 331–347.

Radhakrishna, T., Joseph, M., 1996. Proterozoic paleomagnetism of the mafic dyke swarms in the high grade region of southern India. Precambrian Res. 76, 31–46.

Radhakrishna, T., Chandra, R., Srivastava, A.K., Balasubramonian, G., 2013. Central/Eastern Indian Bundelkhand and Bastar cratons in the Palaeoproterozoic supercontinental reconstructions: a palaeomagnetic perspective. Precambrian Research 226, 91– 104.

Radhakrishna, T., Krishnendu, N.R., Balasubramonian, G. Palaeoproterozoic Indian shield in the global continental assembly: evidences from palaeomagnetism of mafic dykes. Earth-Science Reviews, in press.

Ramakrishnan, M., Vaidyanadhan, R., 2008. Geology of India. Geological Society of India 1, 994.

Ramachandra, H.M., Mishra, V.P., Deshmukh, S.S., 1995. Mafic dykes in the Bastar Precambrian: study of the Bhanupratappur-Keskal mafic dyke swarm. In: Devaraju, T.C. (Ed.), Mafic Dyke Swarms of Peninsular, vol. 33. Geological Society of India Memoir, pp. 183–207.

Ramam, P.K., Murty, V.N., 1997. Geology of Andhra Pradesh. Geological Society of India, Bangalore, 245 pp.

Rao, J.M., Rao, G.V.S.P., Patil, S.K., 1990. Geochemical and paleomagnetic studies on the middle Proterozoic Karimnagar mafic dyke swarm. In: Parker, A.J., Rickwood, P.C., Tucker, D.H. (Eds.), Mafic Dykes and Emplacement Mechanisms, pp. 373–382.

Rao, V.P., Pupper, J.H., 1996. Geochemistry and petrogenesis and tectonic setting of Proterozoic mafic dyke swarms, East Dharwar Craton, India. Journal of Geological Society of India 47, 165–174.

Rogers, J.J.W. (*1986*) The Dharwar craton and the assembly of peninsular India. J. Geol., v. 94, 129–144.

Rogers, J.J., Santosh, M., 2002. Configuration of Columbia, a Mesoproterozoic supercontinent. Gondwana Research 5, 5–22.

Roy, A. and Hanuma Prasad, M. (2003) Tectonothermal events in Central Indian Tectonic Zone and its implications in Rodinian crustal assembly. Jour. Asian Earth Sci., v.22, pp.115–129.

Roy, A., Kagami, H., Yoshida,M., Roy, A., Bandyopadhyay, B.K., Chattopadhyay, A., Khan, A.S., Huin, A.K. and Pal, T. (2006). Rb-Sr and Sm-Nd dating of different metamorphic events from the Sausar Belt, central India: implications for Proterozoic crustal evolution. J. Asian Earth Sci., vol. 26, pp. 61–76.

Saha, D., & Tripathy, V., 2012. Palaeoproterozoic sedimentation in the Cuddapah Basin, south India and regional tectonics: a review. Geological Society, London, Special Publications 365(1), 161-184.

Salminen, J., Pesonen, L.J., Reimold, W.U., Donadini, F., Gibson, R.L., 2009. Paleomagnetic and rock magnetic study of the Vredefort impact structure and the Johannesburg Dome, Kaapvaal Craton, South Africa-Implications for the apparent polar wander path of the Kaapvaal Craton during the Mesoproterozoic. Precambrian Research 168, 167-184.

Salminen, J., Halls, H.C., Mertanen, S., Pesonen, L.J., Vuollo, J., Söderlund, U., 2013. Paleomagnetic and geochronological studies on Paleoproterozoic diabase dykes of Karelia, East Finland—Key for testing the Superia supercraton. Precambrian Research.

Schutts, L. D., and Dunlop, D. J., 1981. Proterozoic magnetic overprinting of Archean rocks in the Canadian Superior Province. Nature (London), 291: 642-645.

Singh, A.P., Mishra, D.C., 2002. Tectonosedimentary evolution of the Cuddapah basin and Eastern Ghats mobile belt (India) as Proterozoic collision: gravity, seismic, and geodynamic constraints. J. Geodyn. 33, 249–267.

Smirnov, A.V., Evans, D.A.D., 2006. Paleomagnetism of the ~2.4 Ga Widgiemooltha 639 dike swarm (Western Australia): Preliminary results: Eos (Transactions, A.G.U), 640 v.87, no. 36, abstract no. GP23A-01.

Smirnov, A. V., Evans, D. A., Ernst, R. E., Söderlund, U., & Li, Z. X., 2013. Trading partners: Tectonic ancestry of southern Africa and western Australia, in Archean supercratons Vaalbara and Zimgarn. Precambrian Research 224, 11-22.

Söderlund, U., Hofmann, A., Klausen, M.B., Olsson, J.R., Ernst, R.C., Persson, P., 2010. Towards a complete magmatic barcode for the Zimbabwe craton: baddeleyite U–Pb dating of regional dolerite dyke swarms and sill complexes. Precambrian Research 183, 388–398.

Srivastava R.K., Hamilton M.A., Jayananda M., 2011. A 2.21 Ga Large Igneous Province in the Dharwar Craton, India. International Symposium: Large Igneous Provinces of Asia; Mantle Plumes and Metallogeny. Abstract Volume, Irkutsk, Russia.

Stein, H.J., Hannah, J.L., Zimmerman, A., Markey, R.J., Sarkar, S.C., Pal, A.B., 2004. A 2.5 Ga porphyry Cu–Mo–Au deposit at Malanjkhand, central India; implications for late Archean continental assembly. Precambrian Research 134, 189–226.

Tauxe, Lisa. Essentials of Paleomagnetism. Los Angeles: University of California Press, 2010.

Torsvik, T.H., Briden, J.C., Smethurst, M.A., 2000. IAPD 2000. Norwegian Geophysical Union.

Van der Voo, R., 1990. The reliability of paleomagnetic data. Tectonophysics, 184(1), 1-9.

Vasudev, V.N., Chadwick, B., Nutman, A.P., Hegde, G.V., 2000. Rapid development of late Archaean Hutti schist belt, northern Karnataka: implications of new field data and SHRIMP zircon ages. Journal of Geological Society, India 55, 529–540.

Venkatesh, A.S., Poornachandra Rao, G.V.S., Prasada Rao, N.T.V., Bhalla, M.S., 1987. Paleomagnetic and geochemical studies on dolerite dykes from Tamil Nadu, India. Precambrian Res. 34, 291–310.

Vuollo, J., Huhma, H., 2005. Paleoproterozoic mafic dykes in NE Finland. In: Lehtinen,M., Nurmi, P.A., Rämö, O.T. (Eds.), Precambrian Geology of Finland – Key to theEvolution of the Fennoscandian Shield. Elsevier Science, B.V., Amsterdam, pp.195–236.

Wiedenbeck, M., Goswami, J.N., Roy, A.B., 1996. Stabilization of the Aravalli Craton of northwestern India at 2.5 Ga: an ion microprobe zircon study. Chemical Geology 129, 325–340.

Yedekar, D.B., Jain, S.C., Nair, K.K.K., 1990. The Central Indian collision suture, Precambrian Central Indian. Geological Survey of India Special Publication 28, 1–27.

Zhang, Shihong, Li, Zheng-Xiang, Evans, David AD, Wu, Huaichun, Li, Haiyan, Dong, Jin, 2012. Pre-Rodinia supercontinent Nuna shaping up: A global synthesis with new paleomagnetic results from North China. Earth and Planetary Science Letters 353, 145-155.

Zhao, G.C., Cawood, P.A., Wilde, S.A., Sun, M., 2002. Review of global 2.1–1.8 Ga orogens: implications for a pre-Rodinia supercontinent. Earth Science Reviews 59,125–162.

Zhao, G.C., Sun, M., Wilde, S.A., Li, S.Z., 2004. A Paleo-Mesoproterozoic supercontinent: assembly, growth and breakup. Earth Science Reviews 67, 91-123.

FIGURE CAPTIONS

Figure 1. Columbia reconstruction according to Zhao et al. (2002, 2004). Dark-shaded cratons (green) have paleomagnetic data available at 1.9 Ga and lighter shaded cratons have no paleomagnetic data (Table 8). Legend: Ak=Akitkan; C=Capricorn; CA=Central Aldan; CITZ=Central Indian Tectonic Zone; E=Eburnean; F=Foxe; K=Ketilidian; KK=Kola-Karelian; Kp=Kaapvaal craton; L=Limpopo; M=Madagascar; NCB=North China Block; NQ=Nugssugtoquidian; P=Pachelma; Pe=Penokean; TA=Transantarctic; Taz=TransAmazonian; TH=Trans-Hudson; TNC=Trans North China; TT=Taltson-Thelon; SAM=South America blocks (Amazonia, Rio de la Plata); SCB=South China Block; Sf=Svecofennian; U=Ungava; V=Volhyn; WAfr=West Africa; W=Wopmay; Zm=Zimbabwe craton.

Figure 2. Generalized geologic map of Peninsular India showing the major cratons and various dyke swarms intruding each craton (modified after Meert et al. 2011). The Dharwar craton (focus of this study) is located in southern peninsular India. The Pullivendla sill is represented by the yellow star. CITZ=Central Indian Tectonic Zone; GR=Godavari Rift; C=Cuddapah Basin; V=Vindhyan Basin; Ch=Chhattisgarh Basin.

Figure 3. Field area for the present study of Dharwar dykes (modified after French and Heaman 2010). The Pullivendla sill was dated by French et al. (2008) to 1885 ± 3.1 Ma. Exact site locations are given in tables 1-4.

Figure 4. Tera-Wasserburg U–Pb concordia diagram for zircon data from dyke I10-19 with a minimum discordant age of 1839 ± 8.3 Ma (this study).

Figure 5. Results of ground magnetic mapping. (a) Orthophoto (Google Earth) of the intersection of the ENE-trending TN and NNW-trending TP dykes. Purple dots show the locations of individual magnetic field readings. Yellow squares represent the locations of paleomagnetic sampling. (b) Perspective view of the sun-shaded magnetic total field (F) map of the area. View is from ENE to best illustrate the linear break in the anomaly associated with the older TN dyke.

Figure 6. Orthogonal vector plots, equal area stereonets and thermal demagnetization behavior for the 2.37, 2.21, and 2.18 Ga dykes of the Dharwar craton showing typical characteristic remanent magnetization directions. **(a)** Thermal demagnetization behavior of sample 1045-3a from the ~2.4 Ga suite of dykes (reverse direction). The sharp drop in intensity (<50%) at 320°C indicates pyrrhotite as a magnetic carrier. **(b)** Thermal demagnetization behavior of sample 1014-7a from the ~2.4 Ga suite of dykes (normal direction). **(c)** Thermal demagnetization behavior of sample 1035-2a from the 2.21 Ga suite of dykes. **(d)** Thermal demagnetization behavior of sample I571-8 from the 2.18 Ga suite of dykes. Solid (open) circles represent projections on the horizontal (vertical) plane in the orthogonal plots while up (down) pointing paleomagnetic directions are indicated by open (closed) circles in the stereoplots.

Figure 7. Curie temperature analysis. **(a)** Sample 1062-5d from the ~2.4 Ga suite of dykes shows a heating Curie temperature (Tc_H) of 563.8°C and cooling Curie temperature (Tc_C) of 557.7°C

with nearly reversible heating-cooling runs. **(b)** Sample 1017-3c from the ~2.2 Ga suite of dykes shows a heating Curie temperature (Tc_H) of 555.2°C and cooling Curie temperature (Tc_C) of 515.1°C. **(c)** Sample 1067-2b from the ~1.9 Ga suite of dykes shows a heating Curie temperature (Tc_H) of 555.8°C and cooling Curie temperature (Tc_C) of 567.5°C.

Figure 8. Isothermal remanence acquisition curves and back-field IRM. **(a)** Samples 1016-8b and 1062-8a are from the ~2.4 Ga suite of dykes. All samples saturate at about 0.1-0.15 T and coercivity of remanence values ranged from 0.1 to 0.12 T. **(b)** Sample 1017-6b is from the 2.21 Ga suite of dykes and sample 1064-8b is from the 2.18 Ga suite of dykes. All samples saturate at about 0.2-0.25 T and coercivity of remanence values were 0.08 T. **(c)** Samples 1018-2b and 1019-5b are from the 1.88 Ga suite of dykes. All samples saturate at about 0.25-0.3 T and coercivity of remanence values ranged from 0.05 to 0.1 T.

Figure 9. (a) Positive baked contact test from the 2.37 Ga suite of dykes (site 14) (reverse direction). **(b)** Positive baked contact test from the 2.18 Ga suite of dykes (normal direction, site 571). **(c)** Positive baked contact test from the 1.88 Ga suite of dykes (site UR). Baked hosts are sampled within one half-width of the dyke, and unbaked hosts are distant samples. Up (down) pointing paleomagnetic directions are indicated by open (closed) circles.

Figure 10. Orthogonal vector plots, equal area stereonets and thermal demagnetization behavior for the 1.88 Ga suite of dykes from the Dharwar craton showing typical characteristic remanent magnetization directions. **(a)** Alternating field demagnetization behavior of sample 1074-8b from the Pullivendla sill. **(b)** Thermal demagnetization behavior of sample 1018-5a. **(c)** Thermal demagnetization behavior of sample 1019-2a that has a minimum discordant age of 1839 ± 8.3 Ma (this study). Solid (open) circles represent projections on the horizontal (vertical) plane in the orthogonal plots while up (down) pointing paleomagnetic directions are indicated by open (closed) circles in the stereoplots.

Figure 11. Galls projection of mean normal and reverse paleomagnetic poles for the 1.88 Ga suite of dykes. Blue squares represent normal poles and red squares represent reversed poles. Ovals represent the cone of 95% confidence about the mean direction. Black ovals represent the mean $\alpha 95$.

Figure 12. (a) Sketch of cross-cutting dykes in Bukkapatnam with sampling locations. BU (Table 1) is the site where the E-W dyke is baked by the NE trending P27m dyke (Table 4). P27m baked and unbaked are part of the same dyke as BU, but sampled about ~50 m from the BU site. Sites 71 and BU (Table 1) of the Great dyke of Penukonda (~50 m and ~150m respectively from the baked outcrop) give the typical ~2.37 Ga steep paleomagnetic direction. **(b)** Baked contact test. Baked hosts are sampled within one half-width of the dyke, and unbaked hosts are distant samples. Up (down) pointing paleomagnetic directions are indicated by open (closed) circles. **(c)** Petrophysical properties. J = magnetization and k = susceptibility. Scale is logarithmic.

Figure 13. Orthogonal projection showing the paleopositions of the Dhawar (blue), Yilgarn (blue), and Superior (red) cratons as well as the Fennoscandian shield (red) at ~2.4 Ga based on

the paleomagnetic poles given in Table 6. Bolded black lines represent the trends of the dykes used for paleomagnetic analysis. Red lines represent the outline of present day continents.

Figure 14. Mollweide projection showing the paleopositions of the Slave (yellow), Superior (red), and Dharwar (purple) cratons at ~2.2 Ga based on the paleomagnetic poles given in Table 7. The Dharwar craton is plotted at both 2.21 Ga and 2.18 Ga for comparison. Bolded black, red, and pink lines represent the trends of the dykes used for paleomagnetic analysis. Outlines (dotted fill) of present day continents are shown for reference.

Figure 15. (a) Paleogeographic reconstruction at ~1.88 Ga based on the paleomagnetic poles given in Table 8. Select orogens are included for comparative purposes to Fig. 1. Legend: Ba=Baltica (dark blue), Ea=East Antarctica (dotted fill), In=India (purple), Kp=Kaapvaal (light blue), La=Laurentia (green), Na=Northern Australia (pink), Si=Siberia (red), Zm=Zimbabwe (orange). The present day continental outline for Australia is shown for reference. Bolded red lines represent the trends of 1.88 Ga Dharwar and Vestfold Hills dykes. East Antarctica is only plotted to show the relationship between dyke trends, and not as an argument for contiguity. **(b)** Columbia reconstruction according to Zhao et al. (2002, 2004). Note: The reconstruction has been rotated 90° in order to compare relative latitudes from the reference point (red star). **(c)** Reconstruction according to Hou et al. (2008). For a full list of abbreviations see Fig. 1.

Figure 16. APW path for the Dharwar craton utilizing the paleopoles from ~ 2.37 Ga to 1.88 Ga (Tables 1-3). The Dharwar craton is shown in purple and Peninsular India is shown in pink. Colored bolded lines within the Dharwar craton represent the trends of the dykes used for paleomagnetic analysis. Blue squares represent the poles and red ovals represent the cone of 95% confidence about the mean direction. The red oval represents a plume center at 1.88 Ga

Table 1. Paleomagnetic results for 2.37 Ga dykes

Site	Slat (°N)	Slong (°E)	B/N	P	D (°)	I (°)	α95	k	Plat (°N)	Plong (°E)	A95	S	Trend	Ref
2*	12.010	77.020	15	N	150.2	-84.0	3.1	150	22.2	70.7			290	1
3+4	11.980	77.030	17	N	50.8	-75.6	7.1	26	-5.6	56.2			300	1
10	11.890	76.950	5	R	29.5	70.2	5.5	196	41.7	99.6			300	1
12	12.040	78.520	8	N	125.8	-71.3	7.6	55	29.6	47.0			290	1
16	12.580	77.980	10	N	39.4	-80.9	6.1	63	-1.3	66.8			276	1
17	12.630	78.070	5	N	186.4	-84.8	13.0	36	22.9	79.3			270	1
18	13.490	76.580	8	N	105.4	-73.7	11.2	25	19.4	45.5			255	1
20	14.310	76.630	5	N	72.8	-76.4	9.5	66	5.6	51.9			270	1
23	13.800	76.910	5	R	35.7	82.4	20.3	15	25.7	86.5			270	1
12	12.660	77.500	6	N	135.1	-84.7	6.4	110	20.0	69.6			270	2
15	12.650	77.420	6	N	72.6	-78.1	7.4	84	5.1	55.6			295	2
16	12.660	77.420	5	N	60.3	-81.2	7.4	109	3.8	62.5			265	2
C	12.110	79.080	3	N	105.2	-74.5	7.4	280	17.9	49.6			300	2,3
D	12.100	78.916	3	N	169.0	-74.0	14.0	32	41.2	71.7			300	3
E	12.110	79.070	6	N	115.0	-75.0	7.0	75	22.3	51.5			30	3
F	12.210	79.080	4	N	125.0	-75.0	9.0	58	26.8	53.4			300	3
T3	12.090	78.920	7	N	129.7	-73.5	2.8	481	29.9	52.0			300	4
D7	12.080	77.890	6	N	105.8	-75.5	5.2	168	18.0	50.2			295	4
T4	12.060	79.010	7	N	114.4	-67.9	9.6	92	24.6	39.8			30	4
T5	12.050	79.030	6	N	306.5	-76.7	4.1	275	-3.4	99.2			NW-SE	4
T7	12.050	79.080	7	N	92.1	-70.7	7.3	69	11.0	43.3			NW-SE	4
T8	12.110	79.100	3	N	121.0	-78.1	11.9	109	29.9	52.0			NW-SE	4
i=A+B*	14.190	77.640	5	N	56.5	-69.5	7.0	53	-7.1	47.4			255	5
ii*	14.180	77.760	3	N	71.9	-72.7	7.5	271	2.8	47.5			250	5
1	12.900	78.200	7	N	170.0	-80.0	5.0	113	32.0	74.3				6
2	12.900	78.200	6	N	88.0	-81.0	6.3	82	11.7	60.3				6
3	12.900	78.200	9	N	127.0	-77.0	4.2	124	26.7	56.2				6
10	12.730	77.520	4	N	141.0	-75.0	10.0	50	33.5	56.6			280	7
Hol [1]	12.790	76.230	4	N	62.2	-78.4	3.0	916	1.8	56.6			310	8
Hol [2]	12.790	76.230	4	N	54.7	-79.2	6.2	218	0.3	59.3			65	8
Dyke 3	18.127	79.220	8	N	68.9	-65.2	11.2	20	0.3	39.9			NE-SW	9
Dyke 2*	17.504	78.869	15	N	102.8	-66.6	6.8	28	21.4	35.5			NE-SW	9
BS1	20.130	81.560	13	R	242.0	69.0	16.6	22	0.3	49.0			NW	10

Table 1. Continued

Site	Slat (°N)	Slong (°E)	B/N	P	D (°)	I (°)	α95	k	Plat (°N)	Plong (°E)	A95	S	Trend	Ref
BS8	19.560	81.710	15	N	138.0	-83.0	19.3	13	29.0	71.0			NW	10
BS13	20.320	81.200	15	R	216.0	84.0	13.9	15	11.0	74.0			NW	10
BS19	20.200	81.350	11	N	176.0	-76.0	9.2	38	47.0	79.0			NW	10
P3*	12.649	77.496	17	N	142.8	-79.3	6.3	33	28.7	63.4			E-W	11
P10	12.470	77.320	4	R	18.0	66.9	7.9	136	50.1	95.5			E-W	11
P16	13.509	76.582	16	N	76.5	-81.8	11.7	11	9.3	60.8			E-W	11
P26	14.075	77.280	4	N	71.4	-66.6	11.9	61	-1.1	38.9			E-W	11
P28	14.197	77.808	4	N	98.2	-68.2	6.9	180	16.2	37.8			E-W	11
P37	12.060	79.350	5	N	197.9	-76.1	2.9	716	36.9	89.2			150	12
P38	12.050	79.330	4	N	174.5	-79.3	9.8	88	32.6	77.0			140	12
P58	12.110	79.250	7	N	174.9	-75.9	6.1	100	38.7	76.3			115	12
P59	12.160	79.160	4	N	302.2	-74.8	9.2	100	3.7	103.0			115	12
P42	12.200	78.900	8	N	130.2	-72.1	4.9	129	31.3	49.0			125	12
P38	14.450	77.700	6	R	196.0	77.0	10.0	42	-9.4	71.0			NW	13
P69	14.570	77.380	6	R	208.6	78.4	18.7	14	-5.2	66.9			NE	13
P53	17.220	80.110	5	R	304.5	85.3	13.0	15	22.3	71.8			NE	13
P78	17.160	79.800	4	N	165.3	-78.7	17.9	27	38.1	72.9			NW	13
P21	14.230	78.750	5	N	23.0	-68.0	9.0	79	-21.7	63.4			E-W	13
2	13.290	76.463	4	N	21.8	-75.8	14.1	43	-11.7	66.6			250	This study
10	13.050	76.800	3	R	48.2	78.5	GC	GC	27.0	95.2			345	This study
14	13.105	76.753	5	N	44.5	-77.7	GC	GC	-4.0	60.4			270	This study
Baked	13.105	76.753	12		161.9	-84.4	10.0	20						This study
Unbaked	13.105	76.753	3		224.2	46.8	73.9	4						This study
16	13.183	77.041	8	N	339.0	-81.0	6.3	78	-3.3	83.3			260	This study
28	13.334	79.405	6	R	256.1	69.5	6.9	95	2.6	43.8			E-W	This study
39	13.541	79.011	4	N	26.7	-72.4	GC	GC	-15.5	64.5			E-W	This study
41	13.540	79.005	6	N	117.4	-78.9	5.1	176	22.4	58.5			E-W	This study
Baked	13.540	79.005	4		2.0	35.2	18.4	26						This study
Unbaked	13.540	79.005	3		9.3	49.9	20.4	38						This study
45	13.533	79.016	5	R	331.0	78.3	6.7	131	32.8	66.3			E-W	This study
62	14.156	78.151	7	N	74.0	-85.0	6.7	80	11.2	68.4			240	This study
71*	14.196	77.810	6	N	75.0	-72.3	4.0	325	4.1	46.4			E-W	This study
590	14.474	77.626	4	N	17.0	-76.0	9.7	90	-10.9	70.0			230	This study

Table 1. Continued

Site	Slat (°N)	Slong (°E)	B/N	P	D (°)	I (°)	α95	k	Plat (°N)	Plong (°E)	A95	S	Trend	Ref
592	14.313	77.637	6	R	234.0	86.0	8.6	42	9.6	71.1			310	This study
596*	14.192	77.796	7	N	85.2	-80.4	5.0	182	11.9	58.8			250	This study
5118	13.255	76.449	7	N	12.0	-81.0	16.0	17	-4.0	72.8			E-W	This study
GR	13.972	77.834	7	R	238.3	72.0	10.5	34	-4.3	50.1			120	This study
TN	14.388	76.920	8	N	116.4	-76.7	13.7	17	24.1	52.2			70	This study
BU*	14.198	77.808	12	N	90.9	-74.9	5.2	71	12.9	48.6			90	This study
Baked	14.198	77.808	1		10.1	-68.1	21.1	35						This study
GT*	14.230	77.632	6	R	259.7	82.2	8.6	61	11.0	62.3			85	This study
Unbaked	14.230	77.630	2		58.6	-20.8	29.5	74						This study
Penukonda			5/32				8.9	75	9.6	47.8				
Mean N			55/384				5.2	15	14.8	60.2				
Mean R			14/92				12.3	11	15.9	69.9				
2.37 Mean	13.719	77.927	18/111		65.0	-81.7	8.3	19	6.6	63.1	8.3	18.8		This study
Combined	16.105	78.970	69/476		88.7	-81.7	4.8	14	15.1	62.2	4.0	18.4		

Notes: Slat=site latitude, Slong=site longitude, B/N=number of sites/samples, Dec=declination, Inc=inclination, α95=cone of 95% confidence about the mean direction, k=kappa precision parameter (Fisher, 1953), Plat = pole latitude, Plong = pole longitude, GC=Great Circle, *=sites with geochronologic ages, A95= radius of the 95% confidence circle about the calculated mean pole, S=scatter of poles. Reference: 1: Halls et al. (2007); 2: Dawson and Hargraves (1994); 3: Venkatesh et al. (1987); 4: Radhakrishna and Joseph (1996); 5: Kumar and Bhalla (1983); 6: Bhalla et al. (1980); 7: Hasnain and Qureshy (1971); 8: Sites from canal cutting at Holenarsipur (A. Kumar, unpublished data, 1985); 9: Kumar et al. (2012a); 10: Radhakrishna et al. (2013a); 11: Piispa et al. (2011); 12: Dash et al. (2013); 13: Radhakrishna et al. (2013b). GT* and i=A+B* = 2454 ±100 Ma (Sm-Nd; none), Zachariah et al. 1995 and 2368.6±1.3 Ma (U-Pb; JEF-99-7), French and Heaman (2010); 2* = 2367±1 Ma (U-Pb *{method}*; 2 *{dating sample name}*), Halls et al. (2007); Dyke 2* = 2367.1±3.1 Ma (U-Pb; Dyke 2), Kumar et al. (2012a); P3* = 2365.4±1.0 Ma (U-Pb; JEF-99-1), French and Heaman (2010); ii*, P28*, 71*, 596* and BU*= 2365.9±1.5 Ma (U-Pb; JEF-99-6), French and Heaman (2010), the Great dyke of Penukonda.

Table 2. Paleomagnetic results for 2.2-2.18 Ga dykes

Site	Slat (°N)	Slong (°E)	B/N	P	D (°)	I (°)	α95	k	Plat (°N)	Plong (°E)	A95	S	Trend	Sw	Ref
AKLD*	13.941	76.977	9/78	N	228.0	-61.0	5.0	95	-40.0	304.0			N-S	2.21	14
dyke ii	12.962	77.376	2/11	N	245.0	-56.0			-28.0	313.0			N-S	2.21	14
dyke iii	16.357	77.725	4/34	N	273.0	-72.0	9.0	98	-12.0	292.0			N-S	2.21	14
P24*	13.537	77.048	9	N	236.3	-47.5	13.7	15	-35.8	321.4			NW-SE	2.21	11
P6	12.498	77.234	5	R	84.8	66.9	25.3	10	-12.8	298.8			N-S	2.21	11
P15	14.368	76.907	6	R	37.5	62.1	15.5	20	-46.8	297.2			NW-SE	2.21	11
17*	13.183	77.041	4	N	218.1	-69.0	5.9	243	-40.4	286.6			NW-SE	2.21	This study
20*	13.061	77.037	8	N	281.9	-46.9	8.9	39	4.1	316.9			N-S	2.21	This study
35	13.547	78.921	8	N	252.6	-61.6	4.9	127	-21.9	307.9			215-35	2.21	This study
SO*	13.488	78.831	4	R	357.8	72.7	13.2	50	-45.4	257.2			315	2.21	This study
TP*	14.387	76.916	6	N	230.3	-57.0	11.9	33	-39.9	309.6			350	2.21	This study
MD	14.045	78.026	9	R	55.0	71.1	7.3	51	-31.0	290.7			120	2.21	This study
Closepet			13/105				21.7	13	-31.4	308.5					
Mean N			8/158				12.1	22	-28.3	306.6				2.21	
Mean R			4/24				25.6	14	-35.1	287.5				2.21	
2.21 Mean	13.724	77.919	6/39		236.1	-67.2	20.1	12	-32.0	297.0	22.0	25.3		2.21	This study
Combined	14.650	77.914	12/182		240.1	-65.5	10.9	17	-30.8	300.7	11.5	20.8		2.21	
P10	12.472	77.319	4		18.0	66.9	7.9	136	-50.1	275.6			E-W	2.18	11
64	14.184	78.163	4		347.2	50.1	13.8	45	69.6	45.1			NW-SE	2.18	This study
568	16.928	77.863	6		9.0	60.0	7.8	76	64.8	94.0			E-W	2.18	This study
571	16.928	77.705	10		3.0	45.0	3.7	171	80.0	93.3			290-110	2.18	This study
Baked			4		23.0	50.2	10.2	83							This study
Unbaked			3		339.0	-42.0	7.0								This study
2.18 Mean	13.700	77.741	4/24		3.2	56.4	17.9	27	67.5	84.5	17.8	15.5		2.18	This study

Notes: Slat=site latitude, Slong=site longitude, B/N=number of sites/samples, Dec=declination, Inc=inclination, α95=cone of 95% confidence about the mean direction, k=kappa precision parameter (Fisher, 1953), Plat = pole latitude, Plong = pole longitude, GC=Great Circle, *=sites with geochronologic ages, A95= radius of the 95% confidence circle about the calculated mean pole, S=scatter of poles. Reference: 11: Piispa et al. (2011); 14: Kumar et al. (2012b). SO* = 2209.3±2.8 Ma (U-Pb; JEF-99-11), French and Heaman (2010); AKLD*, P24*, 17*, 20* and TP* = 2173±43 and 2190±51 Ma (Sm-Nd; HD-14 and HD-10 respectively), Kumar et al. (2012b) and = 2215±2.0 Ma (U-Pb; DC08-12), Srivastava et al. (2011), the Great dyke of Closepet.

Table 3. Paleomagnetic results for 1.88 Ga dykes

Site	Slat (°N)	Slong (°E)	B/N	P	D (°)	I (°)	α95	k	Plat (°N)	Plong (°E)	A95	S	Trend	Ref
532	19.600	81.600	5	N	142.0	25.0	7.0	122	40.0	313.0			NW-SE	15
543	18.900	81.500	14	R	297.0	-24.0	8.0	26	20.4	329.6			N-S	15
524	20.100	81.600	14	N	120.0	5.4	8.0	27	27.0	338.0			NW-SE	15
527	19.800	81.600	9	N	132.1	10.0	7.0	56	37.0	329.0			NW-SE	15
531	19.700	81.600	8	R	292.0	0.5	8.0	54	27.0	341.0			NW-SE	15
Cuddapah Traps	20.000	78.200	15	R	299.0	-6.0	16.0	18	27.0	337.0				16
Cuddapah dyke	14.400	77.700	9	R	317.0	-32.0	25.0	97	37.0	312.0			NE	5
Cuddapah seds	14.600	78.600	76	R	303.0	-5.8	14.4	42	29.3	332.9				17
Cuddapah dyke	13.600	79.300	10	R	296.6	-26.3	50.0	7	21.5	328.2			E-W	18
Tiptur dyke	13.400	76.000	35	R	287.0	-21.0	12.0	21	13.6	331.0				6
BS2	19.830	81.640	15	N	118.0	8.0	7.2	47	25.0	337.0			NW	10
BS7	19.550	81.720	15	R	286.0	-1.0	16.9	17	15.0	346.0			NW	10
BS11	19.630	81.600	14	N	121.0	10.0	11.4	22	27.0	335.0			NW	10
BS14	20.310	81.090	17	N	106.0	14.0	14.9	21	12.0	339.0			NW	10
BS17	20.200	81.500	10	N	101.0	-19.0	13.8	32	14.0	357.0			NW	10
BS18	20.200	81.460	10	N	99.0	-29.0	8.0	58	14.0	003.0			NW	10
P9	12.424	77.234	6	R	304.6	17.3	16.1	13	35.5	349.3			E-W	11
P4	16.760	77.800	5	R	337.8	9.1	16.7	22	65.1	321.1			NW	13
P9	16.450	78.160	6	R	320.1	3.9	23.0	10	49.6	331.9			NW	13
P10	16.230	78.010	6	R	335.7	21.0	15.4	20	65.8	338.3			NW	13
P15	15.210	77.730	8	R	327.1	9.4	16.1	13	56.0	333.2			NW	13
P13b	15.350	77.820	7	R	335.4	-11.5	15.6	16	57.7	308.7			NW	13
P57	14.100	79.260	5	R	320.9	3.1	19.1	17	48.6	331.6			NW	13
P64	16.980	79.070	4	R	308.5	22.8	25.6	14	40.0	350.7			NW	13
P76	16.800	79.700	5	R	320.3	-4.8	19.9	16	46.4	327.4			E-W	13
P1	13.510	79.380	5	R	321.2	-6.2	14.3	30	48.1	328.8			E-W	13
P25	13.790	79.070	8	R	325.6	17.8	15.5	14	56.0	344.9			E-W	13
P39	14.020	78.650	7	R	308.6	-0.1	19.7	11	37.2	337.6			E-W	13
P71	13.580	79.090	5	R	333.2	17.9	17.9	19	63.4	342.4			NE	13
1	13.299	76.459	8	R	344.0	15.0	GC	GC	73.3	328.2			275	This study
18	13.068	77.009	11	N	119.6	7.1	6.1	56	27.8	335.8			330	This study

19*	13.063	77.008	7	R	337.1	-13.9	GC	GC	59.6	306.8			330	This study
26	13.279	79.229	6	R	283.3	-26.5	8.6	61	9.3	332.3			E-W	This study

Table 3. Continued

Site	Slat (°N)	Slong (°E)	B/N	P	D (°)	I (°)	α95	k	Plat (°N)	Plong (°E)	A95	S	Trend	Ref
29	13.334	79.405	6	R	289.7	9.3	6.0	125	20.2	349.5			E-W	This study
31	13.379	79.410	7	N	120.4	46.2	6.1	97	19.2	313.5			255	This study
32	13.417	79.413	4	N	141.8	22.0	GC	GC	44.7	317.9			310	This study
34	13.488	78.831	8	R	287.1	5.4	4.6	147	17.3	347.5			E-W	This study
40	13.541	79.011	5	R	286.3	-22.3	GC	GC	12.7	333.6			E-W	This study
43	13.250	79.100	5	R	295.0	-3.0	13.0	33	24.0	341.0			E-W	This study
66	14.106	78.127	4	R	307.5	-14.9	GC	GC	33.6	328.9			310-130	This study
67	14.138	77.935	3	R	286.2	8.8	9.8	160	16.8	348.3			240	This study
74* Pullivendla sill	14.770	78.172	5	R	314.4	8.0	12.0	42	43.8	339.4			290	This study
86	15.340	77.810	16	R	332.0	-3.0	7.0	27	57.0	316.0			260	This study
87	16.640	77.850	7	R	301.2	5.1	11.9	28	30.6	340.8			310	This study
Baked	16.640	77.850	4		128.0	-6.0	22.0							
Unbaked	16.640	77.850	2		123.0	32.0								
539	18.990	81.610	4	R	330.0	-14.0	6.4	206	51.0	313.0			300	This study
574	16.600	77.900	6	R	308.0	10.0	16.0	20	34.0	330.0			NW-SE	This study
575	16.640	77.850	4	R	286.0	-12.0	10.6	76	13.0	337.0			320	This study
586	15.400	77.800	8	R	306.0	-22.0	6.4	76	30.2	324.4			330	This study
587	15.400	77.800	3	R	321.0	-4.2	29.0	19	48.0	327.0			330	This study
588	15.300	77.800	5	R	315.0	3.1	8.7	79	43.5	335.0			320	This study
597	14.200	77.810	6	R	320.0	-16.0	10.9	39	44.5	320.9			330	This study
5115	13.310	76.460	7	R	296.0	-12.0	13.0	22	24.0	333.0			310	This study
KD site	13.520	78.800	6	R	315.0	-1.0	6.0	139	43.0	335.0			290	This study
UR	14.246	78.079	5	R	324.2	10.1	14.7	28	53.6	337.1			310	This study
Baked	14.246	78.079	1		326.6	-1.3								This study
Unbaked	14.245	78.076	7		13.4	75.2	12.0	26						This study
NM	14.138	77.935	5	R	314.5	18.8	20.3	15	45.3	347.5			60	This study
Baked	14.138	77.935	1		353.7	3.9								This study
Unbaked	14.138	77.935	1		12.5	43.8								This study
MK	13.992	77.990	3	R	286.8	-39.0	19.1	43	9.7	322.2			10	This study
GE	13.973	77.805	3	R	321.0	1.7	13.6	83	49.2	332.4			30	This study
Baked	13.973	77.805	1		10.2	18.2								This study

Unbaked	13.973	77.806	3		16.7	82.3	38.4	11						This study
BX	14.193	77.814	10	R	330.4	-36.1	15.6	11	45.1	298.9			315	This study

Table 3. Continued

Site	Slat (°N)	Slong (°E)	B/N	P	D (°)	I (°)	α95	k	Plat (°N)	Plong (°E)	A95	S	Trend	Ref
Baked	14.198	77.811	5		350.4	-36.6	18.5	18						This study
Unbaked	14.193	77.814	1		352.3	46.2								This study
Mean N			11/116				10.4	20	27.0	335.3				
Mean R			47/414				5.0	18	38.6	333.1				
1.9 Mean	15.707	79.050	29/177		129.3	9.2	6.6	18	35.9	331.2	6.6	19.3		This study
Combined	16.367	78.860	58/530		129.1	4.2	4.5	18	36.5	333.5	5.6	23.4		

Notes: Slat=site latitude, Slong=site longitude, B/N=number of sites/samples, Dec=declination, Inc=inclination, α95=cone of 95% confidence about the mean direction, k=kappa precision parameter (Fisher, 1953), Plat = pole latitude, Plong = pole longitude, GC=Great Circle, *=sites with geochronologic ages, A95= radius of the 95% confidence circle about the calculated mean pole, S=scatter of poles. Reference: 5: Kumar and Bhalla (1983); 6: Bhalla et al. (1980); 10: Radhakrishna et al. (2013a); 11:Piispa et al. (2011); 13: Radhakrishna et al. (2013b); 15: Meert et al. (2011); 16: Clark (1982); 17: Prasad et al. (1984); 18: Hargraves and Bhalla (1983). 19* = 1847±6 Ma and 1839±8 Ma (U-Pb; 19), This study; 74* Pullivendla sill = 1885.4±3.1 Ma (U-Pb; JEF-99-9), French et al. (2008).

Table 4. Cuddapah swarm

Site	Slat (°N)	Slong (°E)	B/N	D (°)	I (°)	α95	K	Plat (°N)	Plong (°E)	A95	S	Trend	Ref
Component S^	14.162	76.983	4/43	56.0	-15.0	42.0	6	30.3	184.8			NW-SE	14
Dyke 1^	18.210	78.820	9	63.4	-5.8	15.9	9	24.1	181.0			NW-SE	9
Karimnagar^	18.451	79.152	12	52.5	-24.5	8.7	22	31.9	197.0			NW-SE	19
P18^	13.402	76.606	6	82.0	-18.7	4.9	188	5.4	180.0			NW-SE	11
Dyke iii	14.194	77.806	3/12	63.7	-7.3	5.8	453	24.4	178.6			NW-SE	5
Dyke iv	14.187	77.735	2/9	57.0	-8.0	15.7	254	30.6	181.3			NE-SW	5
P2^	16.830	77.590	7	48.0	-25.5	14.9	18	33.8	197.2			NE	13
P3^	16.820	77.710	7	35.7	6.8	17.9	12	52.5	184.7			NE	13
P12^	16.280	78.010	6	58.4	4.1	16.1	18	30.9	175.4			NW	13
P35^	16.520	78.050	5	33.8	11.8	13.4	34	55.3	181.8			NW	13
P19^	14.610	77.800	5	58.4	9.3	14.8	28	31.8	171.4			NE	13
P37^	14.500	77.770	7	44.2	5.5	10.9	32	44.9	178.6			NE	13
P68^	14.750	77.510	7	63.0	-12.0	13.0	21	24.2	181.3			NW	13
P13a^	15.350	77.820	4	24.3	-4.4	19.6	23	60.2	201.9			NW	13
P62^	16.720	79.180	5	23.0	-4.1	17.7	20	60.5	206.6			NS	13
P63^	16.690	79.020	6	21.7	-15.1	11.2	37	57.5	216.0			NS	13
P66^	17.210	79.160	6	49.7	16.7	19.0	14	40.9	172.8			NW	13
P79^	17.170	79.360	8	15.8	-6.0	13.6	18	64.5	220.2			NS	13
P44^	17.310	79.680	5	64.0	24.0	17.0	21	28.2	164.5			NS	13
P29	13.400	79.440	4	63.9	20.6	18.9	25	27.6	164.3			EW	13
P40^	14.050	78.700	5	43.9	26.9	17.2	21	47.5	162.8			NW	13
P70^	14.160	78.610	4	60.6	-19.7	11.9	61	25.2	187.2			NE	13
I594^	14.100	77.400	14	46.0	5.1	7.6	28	45.0	177.0				20
I589^	14.100	77.400	8	241.0	-6.4	9.4	36	29.0	171.0				20
I5103^	14.100	77.400	7	79.0	1.3	18.1	12	11.0	169.0			E-W	20
P27m	14.196	77.808	14	65.9	-10.9	6.5	39	21.8	179.8			NE-SW	11
*Baked**	14.197	77.810	4	76.1	-9.0	4.4	445	12.3	175.8			E-W	This study
*Unbaked**	14.197	77.810	4	62.3	-59.1	20.6	37	-6.9	36.8			E-W	This study
P27m+dyke iii^	14.195	77.807	5/26	64.2	-8.2	4.3	468	23.8	178.9			NE-SW	This study
P29	14.181	77.729	4	66.5	-1.4	11.9	61	22.6	174.5			NE-SW	11
Baked	14.181	77.729	1	65.0	14.0								This study

Site	Slat (°N)	Slong (°E)	B/N	D (°)	I (°)	α95	K	Plat (°N)	Plong (°E)	A95	S	Trend	Ref
Unbaked	14.181	77.729	1	18.7	32.0								This study
P29+dyke iv^	14.184	77.732	3/13	60.2	-5.8	11.6	115	28.0	178.9			NE-SW	This study

Table 4. Continued

Site	Slat (°N)	Slong (°E)	B/N	D (°)	I (°)	α95	K	Plat (°N)	Plong (°E)	A95	S	Trend	Ref
MG^	14.259	78.060	4	63.0	-10.1	14.6	40	24.6	180.6			E-W	This study
SB^	14.105	77.771	3	64.5	-16.6	10.9	129	22.1	183.2			NE-SW	This study
SC^	14.092	77.770	3	62.6	13.8	14.9	69	28.2	167.3			NE-SW	This study
Cuddapah Mean	14.176	77.895	11/49	62.9	-5.4	11.0	50	25.4	177.9	5.8	6.1	NE-SW	This study
Combined	15.349	78.151	37/214	52.2	-1.5	6.3	20	35.9	180.6	6.3	18.3		

Notes: Slat=site latitude, Slong=site longitude, B/N=number of sites/samples, Dec=declination, Inc=inclination, α95=cone of 95% confidence about the mean direction, k=kappa precision parameter (Fisher, 1953), Plat = pole latitude, Plong = pole longitude, GC=Great Circle, *=sites with geochronologic ages, A95= radius of the 95% confidence circle about the calculated mean pole, S=scatter of poles, ^=Dykes used for calculation of the grand mean, bold=Dykes used for calculation of Cuddapah mean. Reference: 5: Kumar and Bhalla (1983); 9: Kumar et al. (2012a); 11: Piispa et al. (2011); 13: Radhakrishna et al. (2013b); 14: Kumar et al. (2012b); 19: Rao et al. (1990); 20: Pradhan et al. (2010). Component S* = Secondary overprint in the Great dyke of Closepet with ages 2173±43 and 2190±51 Ma (Sm-Nd; HD-14 and HD-10 respectively), Kumar et al. (2012b) and = 2215±2.0 Ma (U-Pb; DC08-12), Srivastava et al. (2011); Dyke 1* = Secondary overprint in 2368.5±2.6 Ma (U-Pb; Dyke 1), Kumar et al. (2012a); Baked* and Unbaked* = 2365.9±1.5 Ma (U-Pb; JEF-99-6), French and Heaman (2010), the Great Dyke of Penukonda.

Table 5. Geochronological results

Grain Name	$^{207}Pb/^{235}U$	2σ	$^{206}Pb/^{238}U$	2σ	(error corr.)	$^{207}Pb/^{206}Pb$	2σ	$^{206}Pb/^{238}U$ (Age) Ma	*2σ	$^{207}Pb/^{235}U$ (Age) Ma	*2σ	207Pb/ 206Pb (Age) Ma	*2σ
I10-19_1 (core)	4.90861	3.4	0.31526	3.4	0.99	0.11293	0.32945938	1768	52	1803	28	1847	6.0
I10-19_2 (core)	4.65324	3.9	0.30015	3.8	0.99	0.11244	0.46116253	1693	57	1759	32	1839	8.3
I10-19_3 (rim)	1.50094	5.5	0.14266	5.5	0.98	0.07631	0.74018802	860	44	931	33	1103	15

Table 6. Ca. 2.4 Ga paleomagnetic studies.

Pole name	Cont./Craton	Plat (°N)	Plong (°E)	A95	Age	Reference
Karelian dykes	Baltica	10	256	-	2.45 Ga	Mertanen et al. (1999)
Matachewan dykes	Superior	-52	240	2.4°	2.45 Ga	Evans and Halls (2010)
Widgiemooltha	Yilgarn	-10	159	7.5°	2.42 Ga	Smirnov et al. (2013); Evans (1968)
Dharwar dykes	Dharwar	15	62	4.0°	2.37 Ga	This study

Table 7. Ca. 2.2 Ga paleomagnetic studies.

Pole name	Craton	Plat (°N)	Plong (°E)	A95 (dp/dm)	Age	Reference
Malley dykes	Slave	-51	310	(6/8°)	2.23 Ga	Buchan et al. (2012)
Dharwar dykes (2.21)	Dharwar	31	121	11°	2.21 Ga	This study
Dharwar dykes (2.18)	Dharwar	68	85	18°	2.18 Ga	This study
Tulemalu	Rae	-1	122	(6/10°)	~2.19 Ga	Fahrig et al. (1984)
Senneterre	Superior	15	104	(4/7°)	~2.22 Ga	Buchan et al. (1993)

Table 8. Ca. 1.88 Ga paleomagnetic studies.

Pole name	Cont./Craton	Plat (°N)	Plong (°E)	A95	Age	Reference
Mean Baltica	Baltica	41	233	5.0°	1.88 Ga	Pesonen et al. (2003)
Akitkan Group	Siberia	-31	99	-	1.87 Ga	Didenko et al. (2009)
Mashonaland Sills	Zimbabwe	8	338	5.1°	1.88 Ga	Letts et al. (2011)
Molson dykes-B+C2	Superior	29	218	3.8°	1.87 Ga	Halls and Heaman (2000), Zhai et al. (1994); recalc. (Evans and Halls 2010)
Ghost dykes	Slave	0	190		1.88 Ga	Buchan (p.comm)
Post-Waterberg	Kaapvaal	9	15	14.0°	1.87 Ga	Hanson et al. (2004), de Kock (2007)
Black Hills	Kaapvaal	9	352	5.0°	1.88 Ga	Lubina et al. (2010)
Dharwar dykes	India	37	334	5.6°	1.88 Ga	This study
Plum Tree volcanics	Australia	-29	195	14.0°	1.82 Ga	Idnurm and Giddings (1988)

- A radiating dyke swarm is confirmed within the Indian subcontinent at 1.88 Ga
- Paleomagnetic data from India at 1.88 Ga conflict with archetypal Columbia
- We report positive baked contact tests at 2.37, 2.18 and 1.88 Ga
- A combined 2.37 Ga dataset represents one of the most robust for the Paleoproterozoic
- We propose that NE directions are related to Cuddapah basin initiation at 2.1 Ga

- A radiating dyke swarm is confirmed within the Indian subcontinent at 1.88 Ga
- Paleomagnetic data from India at 1.88 Ga conflict with archetypal Columbia
- We report positive baked contact tests at 2.37, 2.18 and 1.88 Ga
- A combined 2.37 Ga dataset represents one of the most robust for the Paleoproterozoic
- We propose that NE directions are related to Cuddapah basin initiation at 2.1 Ga

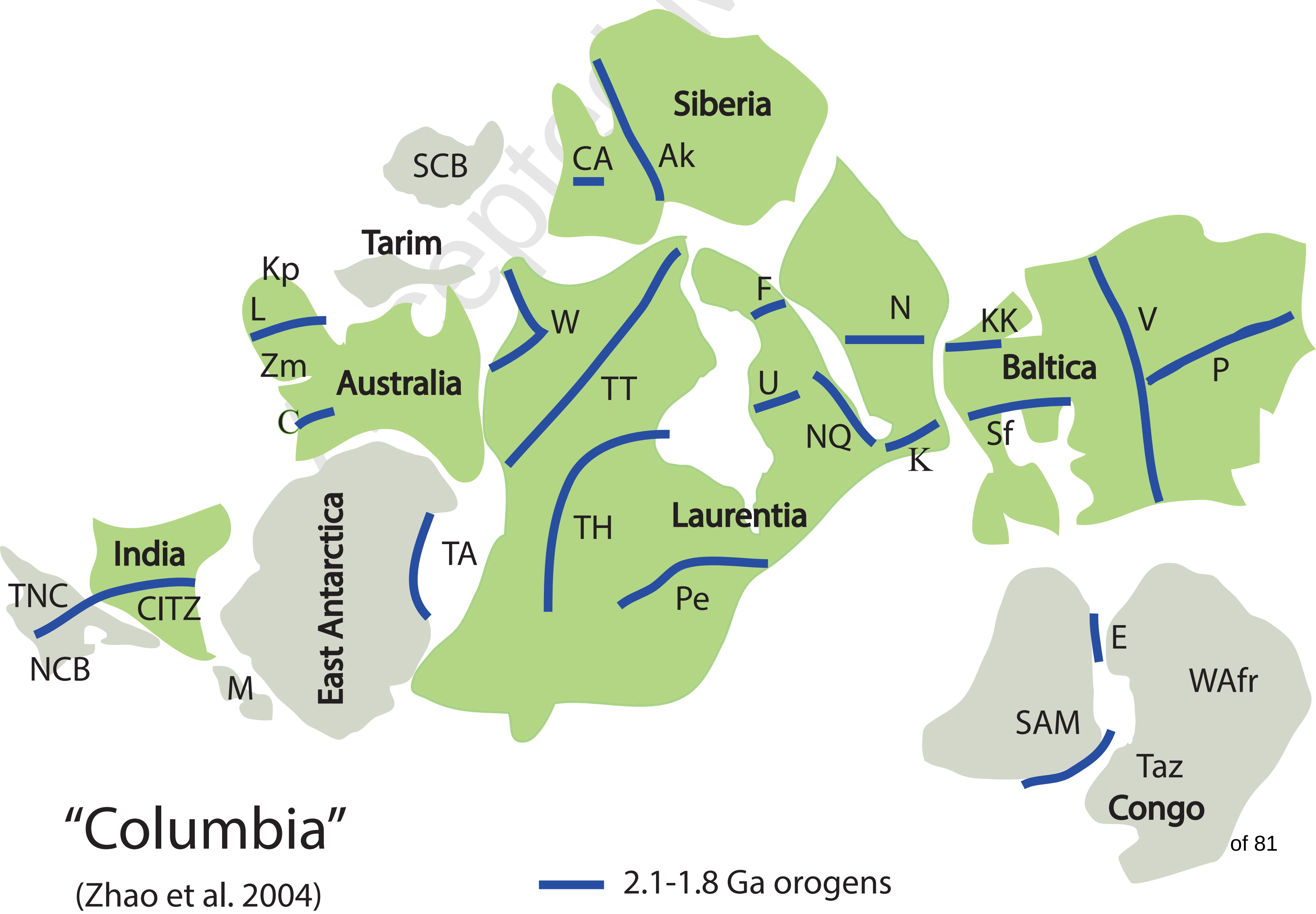
Siberia
SCB
CA
Ak
Tarim
Kp
L
Zm
Australia
C
W
TT
F
N
KK
V
Baltica
P
U
NQ
K
Sf
India
TNC
CITZ
NCB
M
East Antarctica
TA
TH
Laurentia
Pe
E
WAfr
SAM
Taz
Congo
"Columbia"
(Zhao et al. 2004)
2.1-1.8 Ga orogens

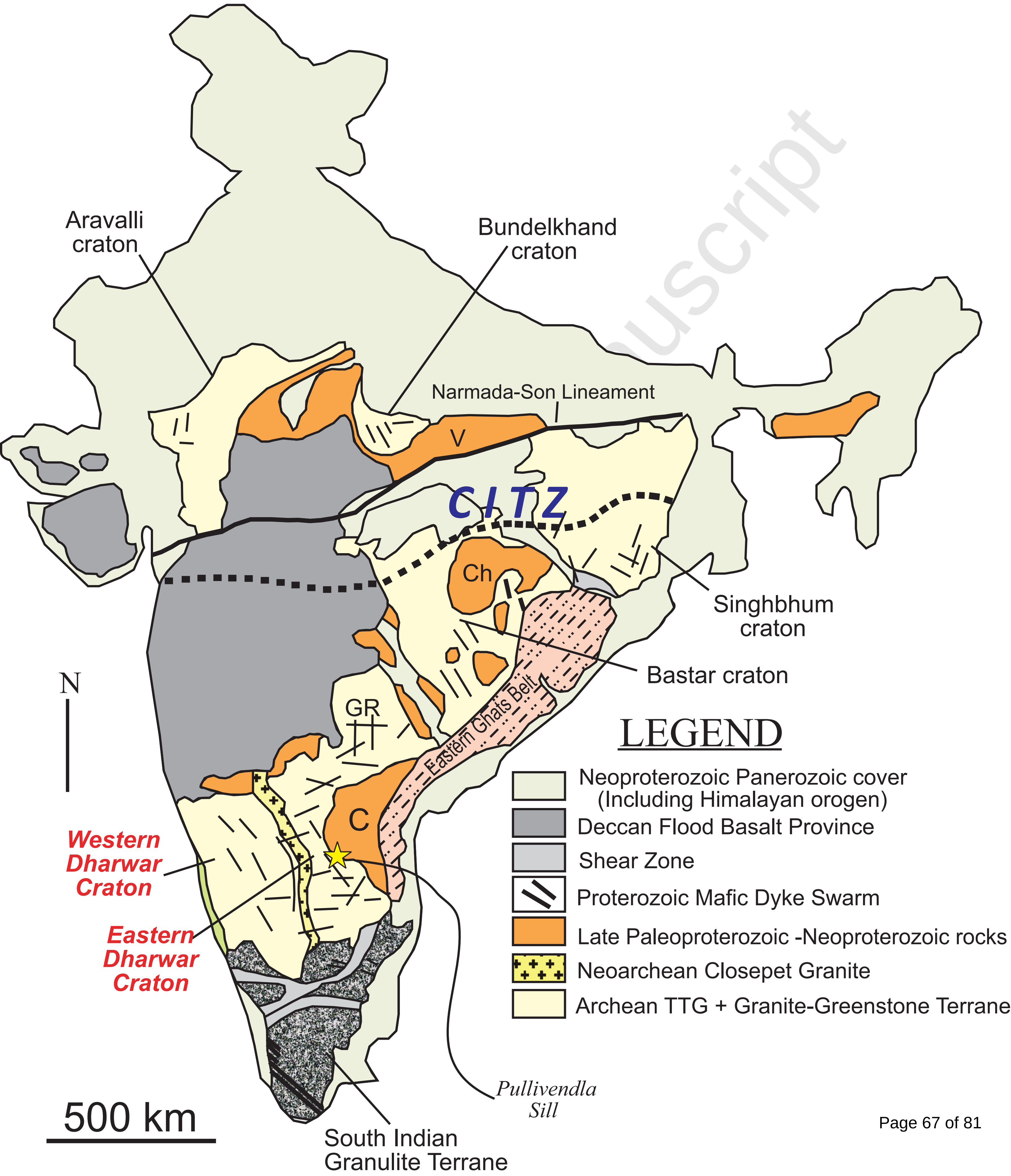
Aravalli craton
Bundelkhand craton
Narmada-Son Lineament
V
CITZ
Ch
Singhbhum craton
Bastar craton
Eastern Ghats Belt
GR
C
N
Western Dharwar Craton
Eastern Dharwar Craton
Pullivendla Sill
South Indian Granulite Terrane
500 km
LEGEND
Neoproterozoic Panerozoic cover (Including Himalayan orogen)
Deccan Flood Basalt Province
Shear Zone
Proterozoic Mafic Dyke Swarm
Late Paleoproterozoic -Neoproterozoic rocks
Neoarchean Closepet Granite
Archean TTG + Granite-Greenstone Terrane

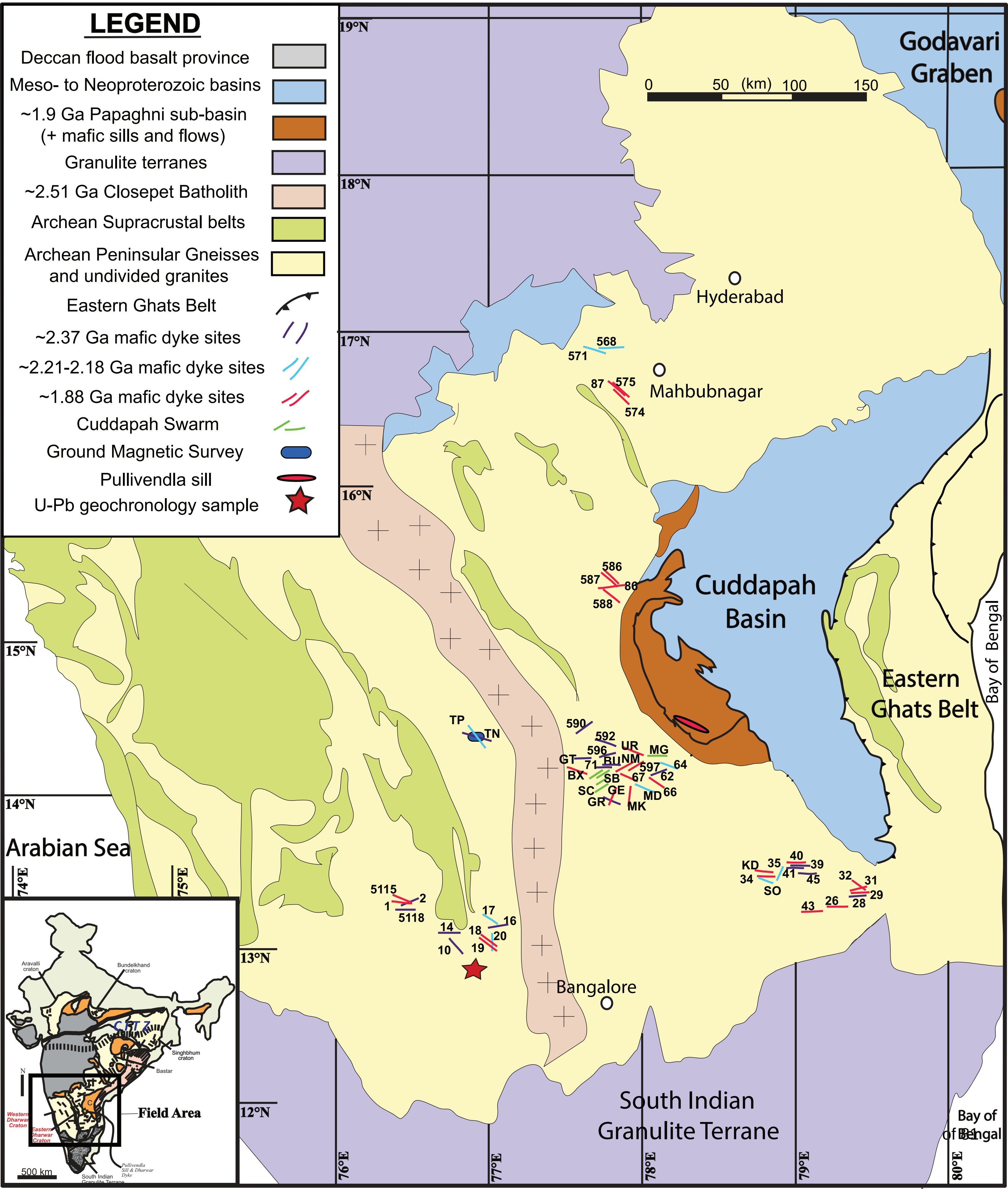
LEGEND
Deccan flood basalt province
Meso- to Neoproterozoic basins
~1.9 Ga Papaghni sub-basin (+ mafic sills and flows)
Granulite terranes
~2.51 Ga Closepet Batholith
Archean Supracrustal belts
Archean Peninsular Gneisses and undivided granites
Eastern Ghats Belt
~2.37 Ga mafic dyke sites
~2.21-2.18 Ga mafic dyke sites
~1.88 Ga mafic dyke sites
Cuddapah Swarm
Ground Magnetic Survey
Pullivendla sill
U-Pb geochronology sample
Godavari Graben
0 50 (km) 100 150
19°N
18°N
17°N
16°N
15°N
14°N
13°N
12°N
74°E
75°E
76°E
77°E
78°E
79°E
80°E
Hyderabad
Mahbubnagar
Cuddapah Basin
Eastern Ghats Belt
Bay of Bengal
Arabian Sea
Bangalore
South Indian Granulite Terrane
568
571
87
575
574
586
587
86
588
590
592
596
UR
MG
GT
71
BU
NM
597
64
BX
SB
67
62
SC
GE
MD
66
GR
MK
TP
TN
KD
35
40
39
34
41
45
SO
32
31
29
28
26
43
5115
2
1
5118
17
16
14
18
20
10
19
Aravalli craton
Bundelkhand craton
CITZ
Singhbhum craton
Bastar
Field Area
Western Dharwar Craton
Eastern Dharwar Craton
500 km
Pullivendla Sill & Dharwar Dyke
South Indian Granulite Terrane

Figure 4

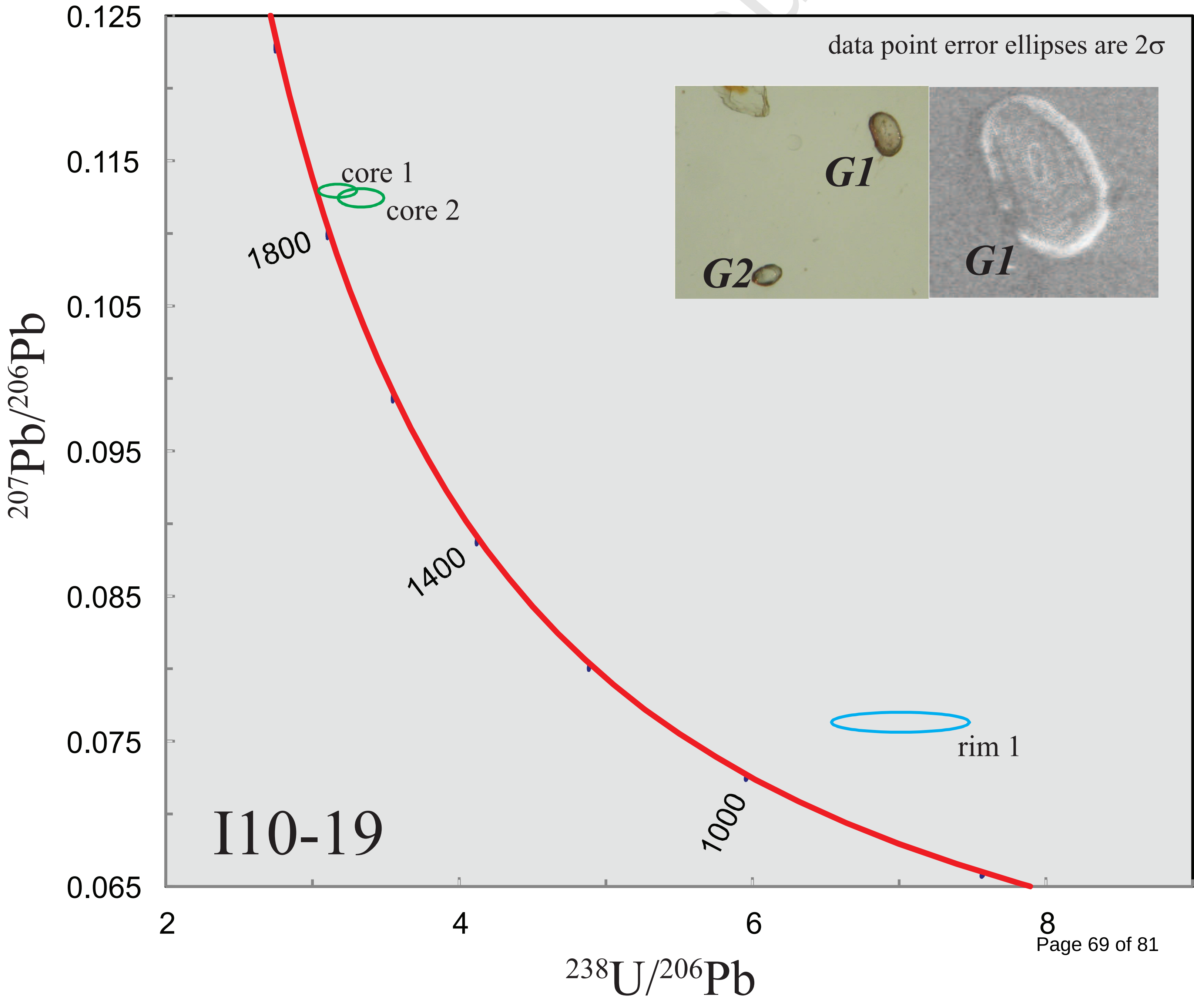

0.125
0.115
0.105
0.095
0.085
0.075
0.065
$^{207}Pb/^{206}Pb$
2
4
6
8
$^{238}U/^{206}Pb$
data point error ellipses are 2σ
core 1
core 2
rim 1
1800
1400
1000
G1
G2
G1
I10-19

Figure 5

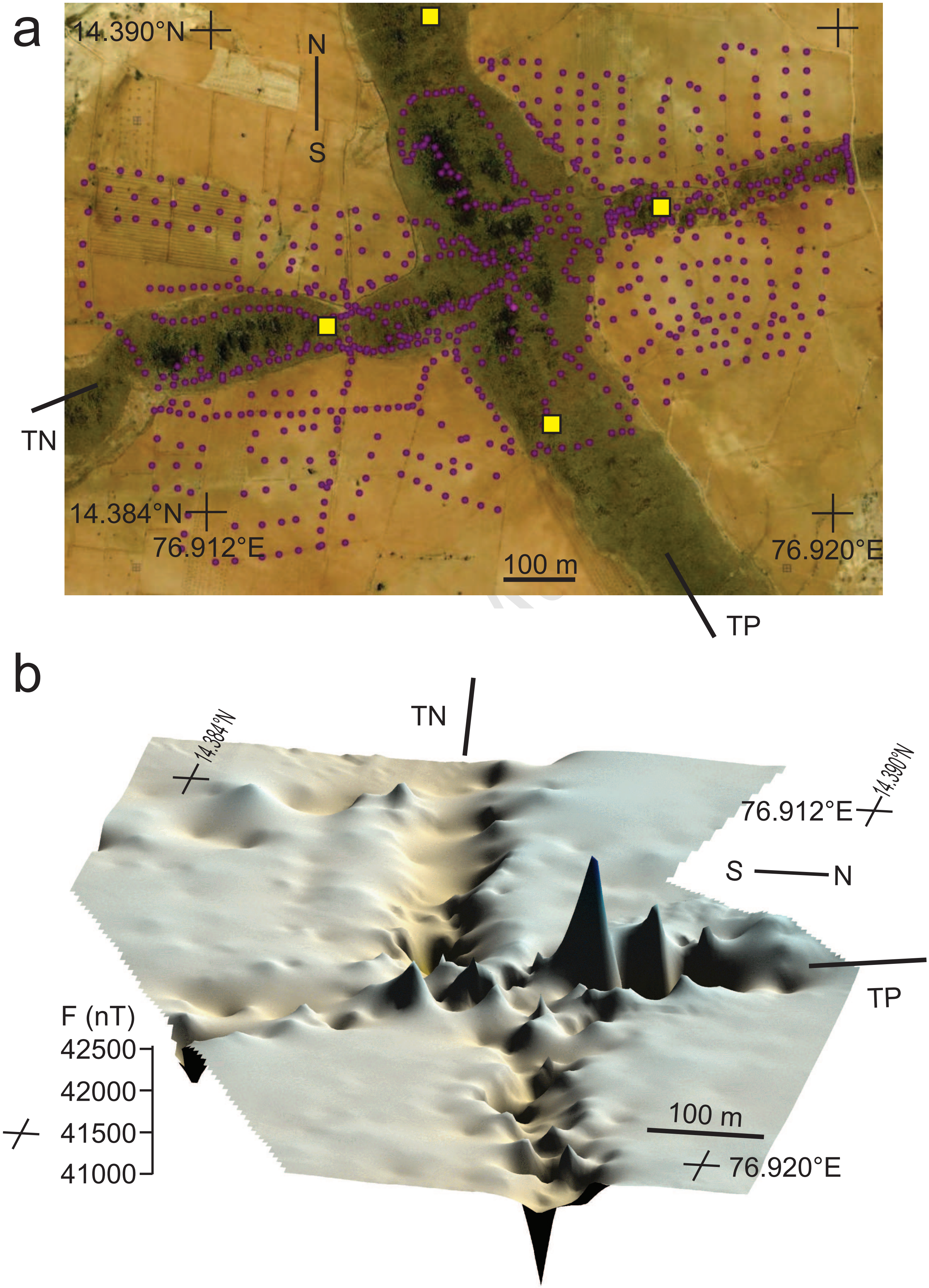

a
14.390°N
N
S
TN
14.384°N
76.912°E
100 m
76.920°E
TP
b
TN
14.384°N
14.390°N
76.912°E
S
N
TP
F (nT)
42500
42000
41500
41000
100 m
76.920°E

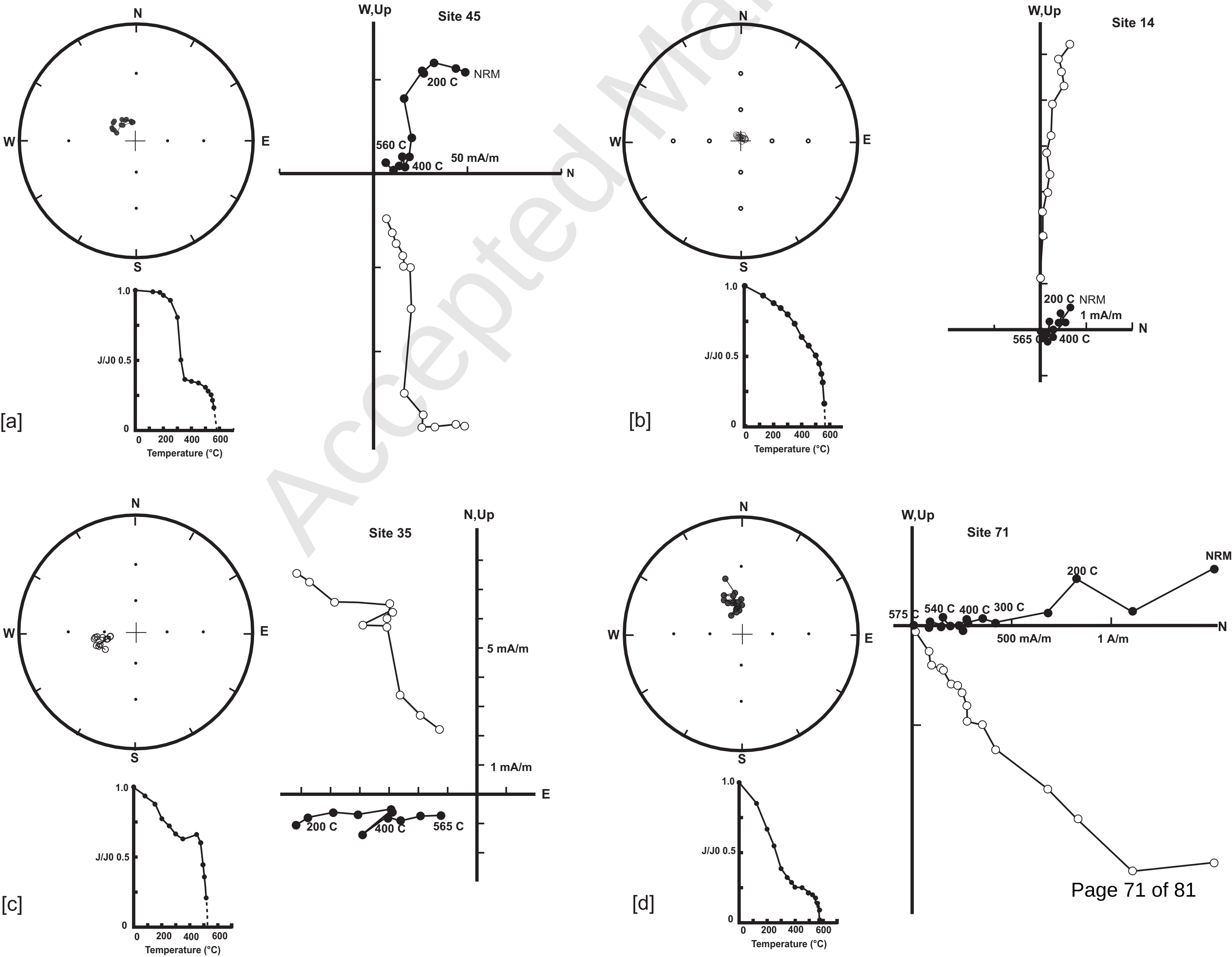
N
W
E
S
W,Up
Site 45
NRM
200 C
560 C
400 C
50 mA/m
N
1.0
J/J0 0.5
0
0 200 400 600
Temperature (°C)
[a]
N
W
E
S
W,Up
Site 14
200 C NRM
1 mA/m
565 C
400 C
N
1.0
J/J0 0.5
0
0 200 400 600
Temperature (°C)
[b]
N
W
E
S
N,Up
Site 35
5 mA/m
1 mA/m
E
200 C
400 C
565 C
1.0
J/J0 0.5
0
0 200 400 600
Temperature (°C)
[c]
N
W
E
S
W,Up
Site 71
NRM
200 C
575 C
540 C
400 C
300 C
500 mA/m
1 A/m
N
1.0
J/J0 0.5
0
0 200 400 600
Temperature (°C)
[d]

Figure 7

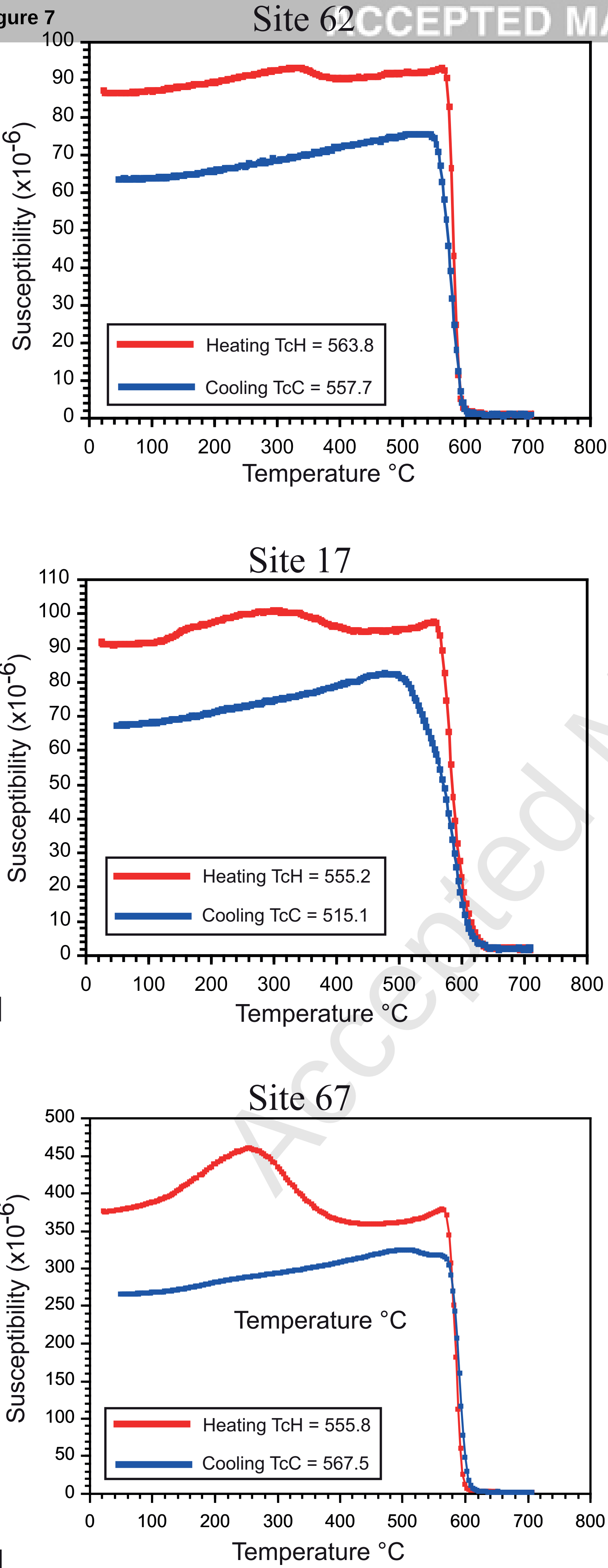
Site 62
Susceptibility (x10^{-6})
Temperature °C
Heating TcH = 563.8
Cooling TcC = 557.7
Site 17
Susceptibility (x10^{-6})
Temperature °C
Heating TcH = 555.2
Cooling TcC = 515.1
Site 67
Susceptibility (x10^{-6})
Temperature °C
Temperature °C
Heating TcH = 555.8
Cooling TcC = 567.5

[a]

[b]

[c]

Figure 8

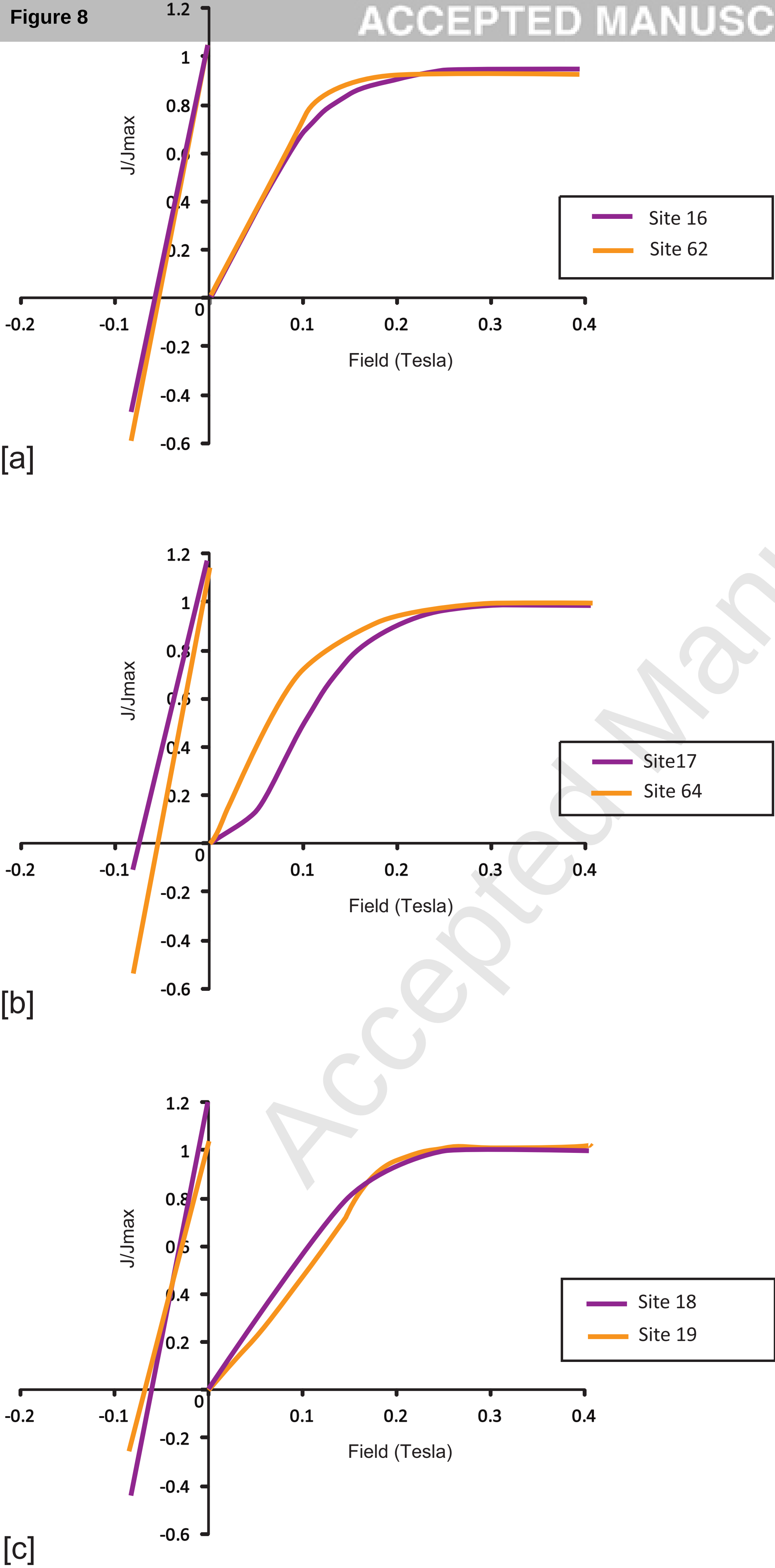
[a]
J/Jmax
Field (Tesla)
Site 16
Site 62
[b]
J/Jmax
Field (Tesla)
Site17
Site 64
[c]
J/Jmax
Field (Tesla)
Site 18
Site 19

Figure 9

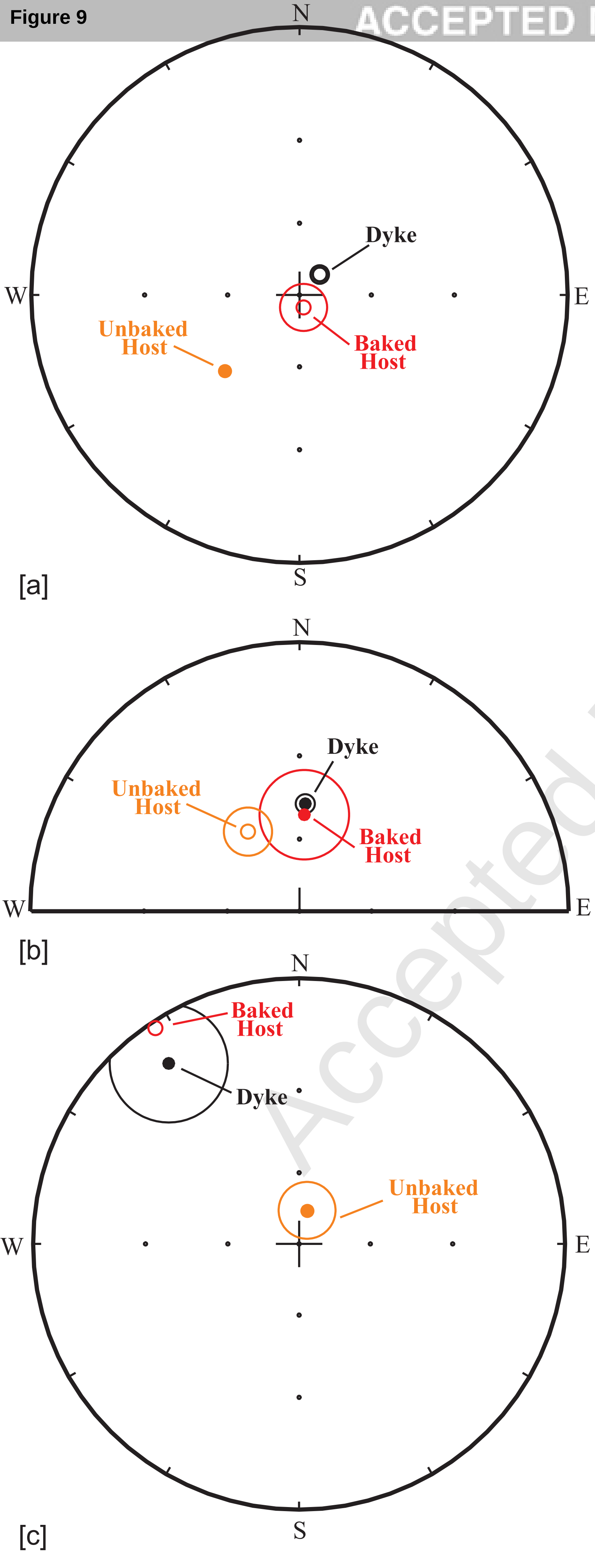

N
W
E
S
Dyke
Unbaked Host
Baked Host
[a]
N
W
E
Dyke
Unbaked Host
Baked Host
[b]
N
W
E
S
Baked Host
Dyke
Unbaked Host
[c]

Figure 10

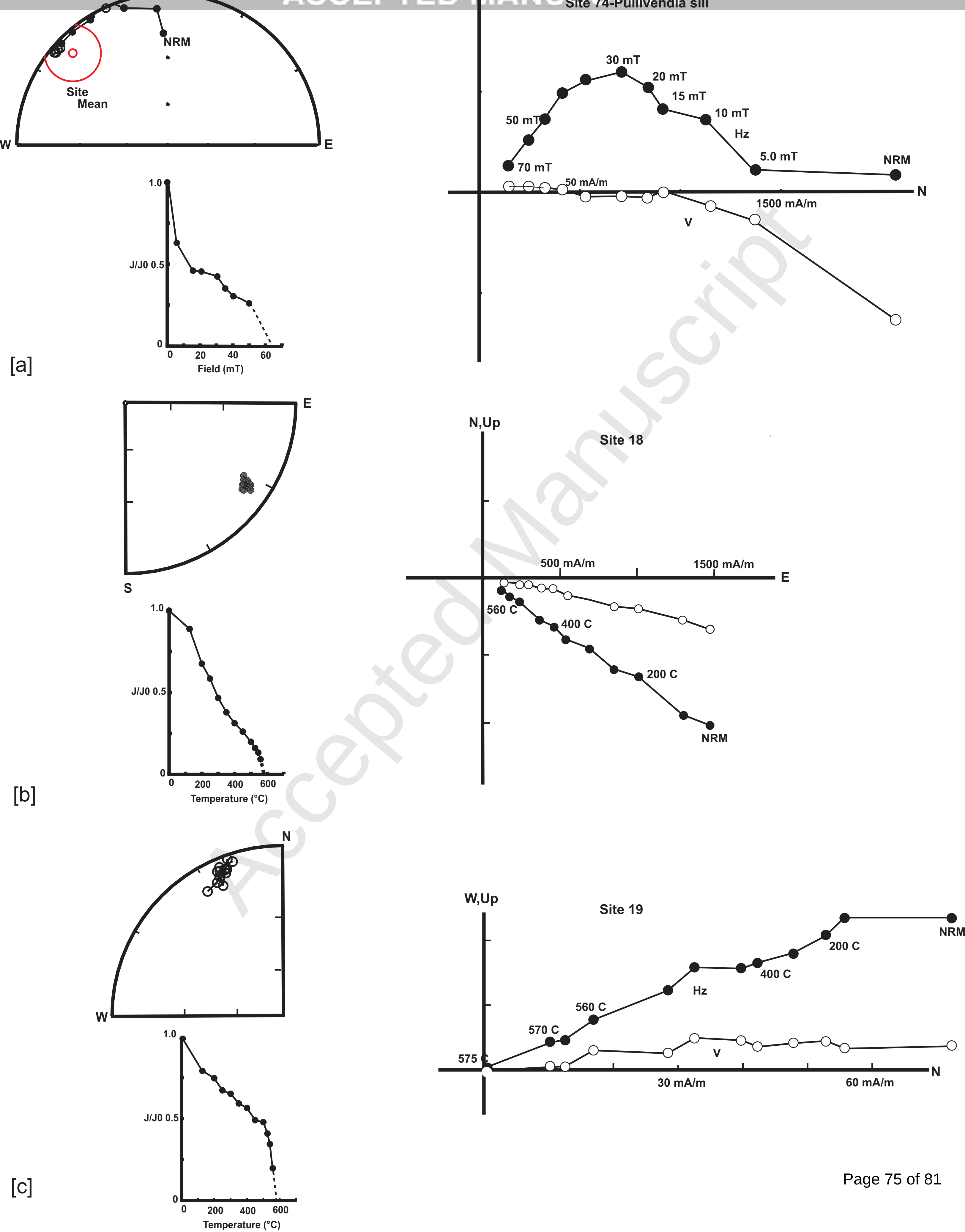
N
NRM
Site
Mean
W
E
1.0
J/J0 0.5
0
0
20
40
60
Field (mT)
[a]
W,Up
Site 74-Pullivendla sill
30 mT
20 mT
15 mT
10 mT
Hz
50 mT
70 mT
5.0 mT
NRM
50 mA/m
N
1500 mA/m
V
E
S
1.0
J/J0 0.5
0
0
200
400
600
Temperature (°C)
[b]
N,Up
Site 18
500 mA/m
1500 mA/m
E
560 C
400 C
200 C
NRM
N
W
1.0
J/J0 0.5
0
0
200
400
600
Temperature (°C)
[c]
W,Up
Site 19
NRM
200 C
400 C
Hz
560 C
570 C
575 C
V
N
30 mA/m
60 mA/m

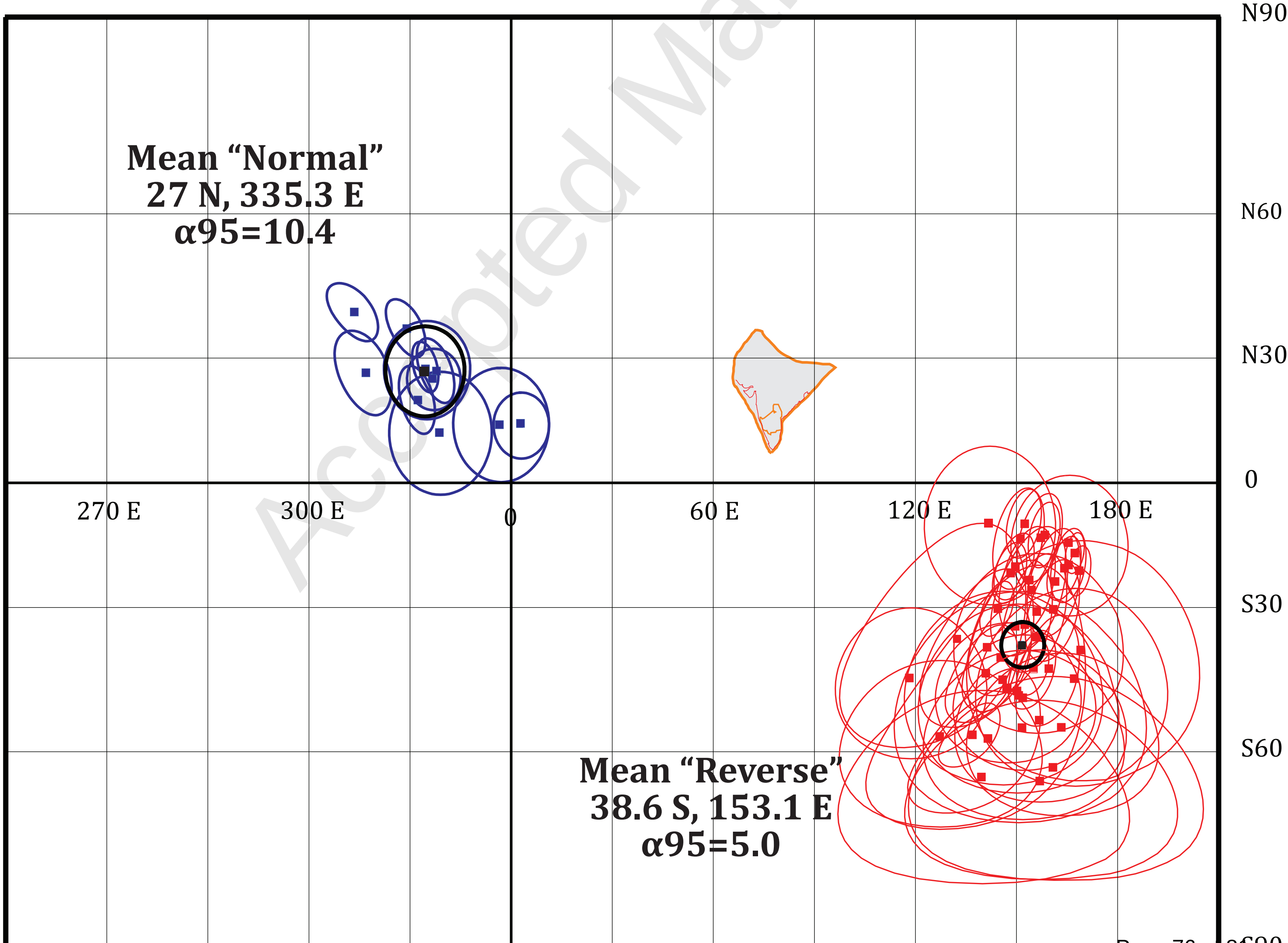
Mean "Normal"
27 N, 335.3 E
α95=10.4
Mean "Reverse"
38.6 S, 153.1 E
α95=5.0
N90
N60
N30
0
S30
S60
S90
270 E
300 E
0
60 E
120 E
180 E

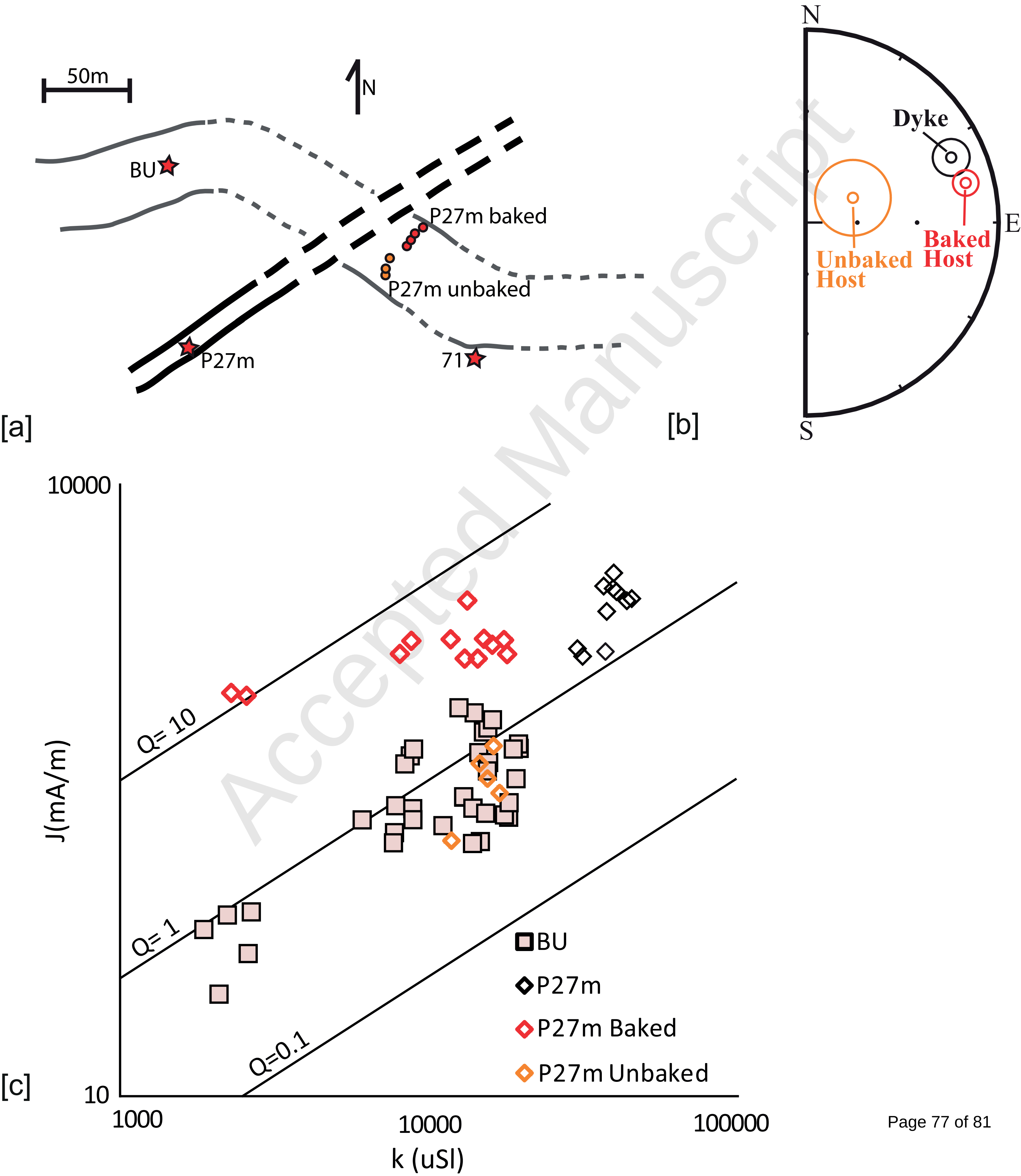
50m
N
BU
P27m baked
P27m unbaked
P27m
71
[a]
N
Dyke
E
Baked Host
Unbaked Host
S
[b]
10000
Q= 10
Q= 1
Q=0.1
J(mA/m)
BU
P27m
P27m Baked
P27m Unbaked
[c]
10
1000
10000
100000
k (uSI)

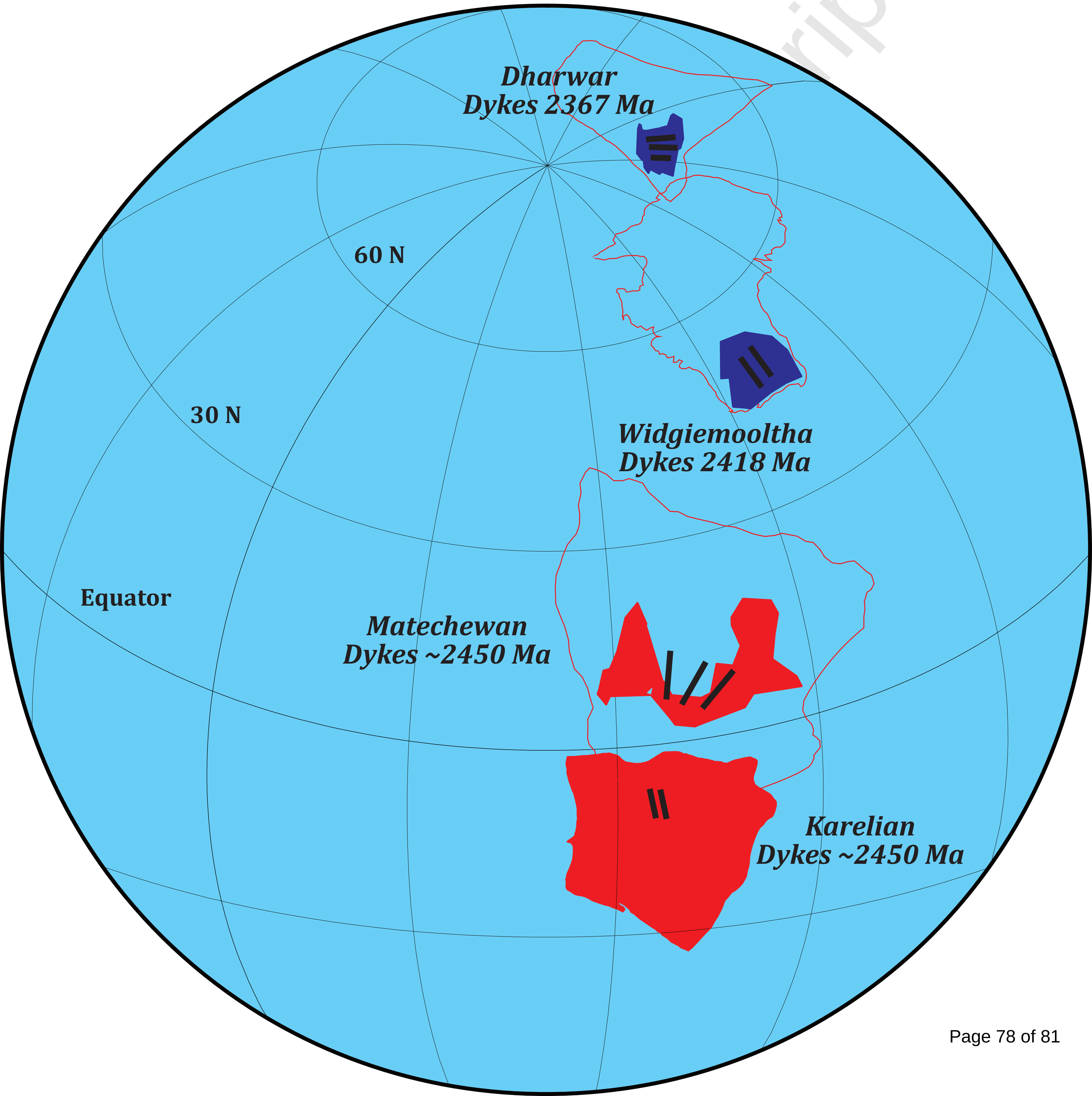
Dharwar
Dykes 2367 Ma
60 N
30 N
Widgiemooltha
Dykes 2418 Ma
Equator
Matechewan
Dykes ~2450 Ma
Karelian
Dykes ~2450 Ma

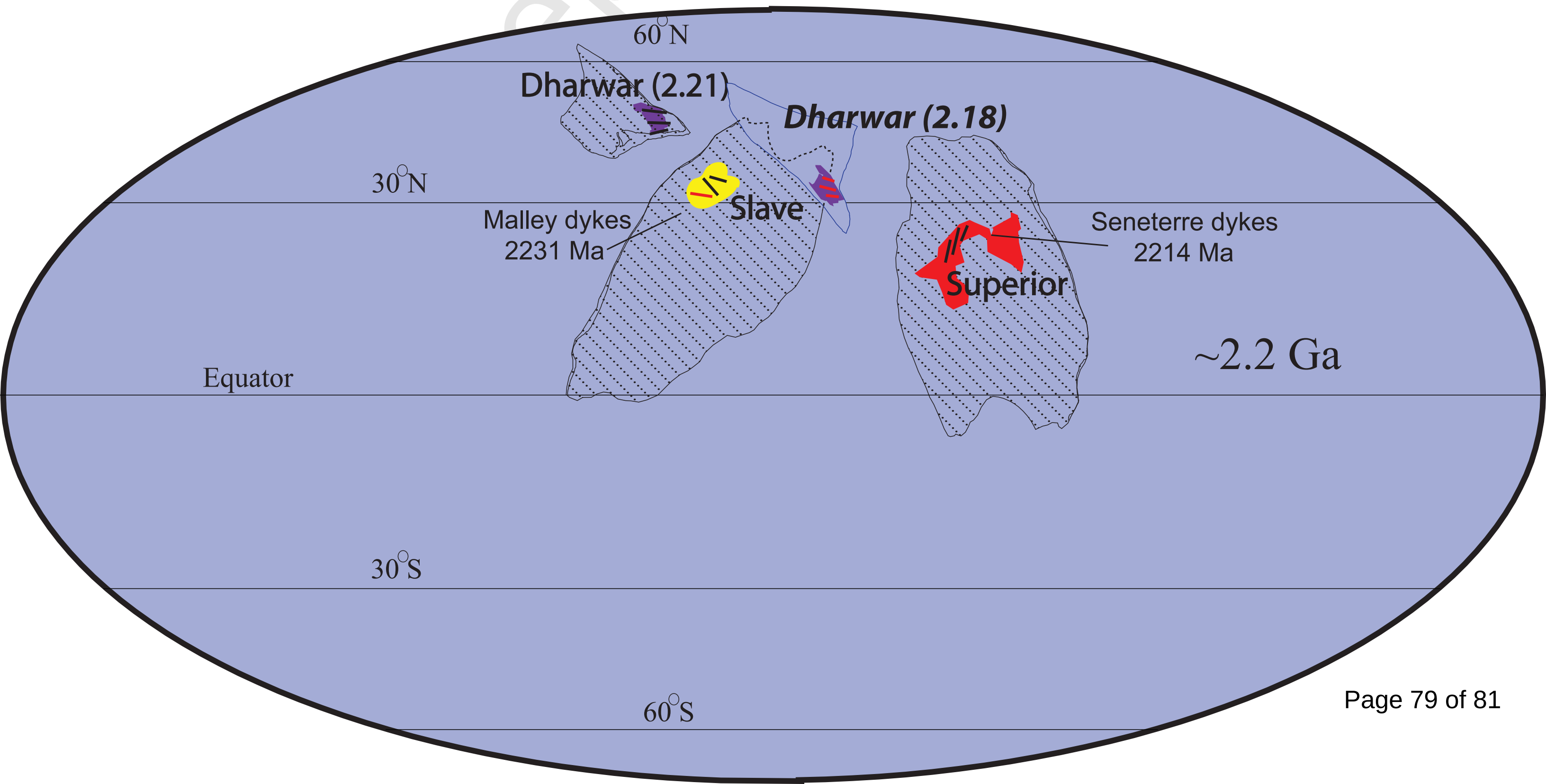
60°N
Dharwar (2.21)
Dharwar (2.18)
30°N
Slave
Malley dykes
2231 Ma
Seneterre dykes
2214 Ma
Superior
~2.2 Ga
Equator
30°S
60°S

Figure 15

[a]

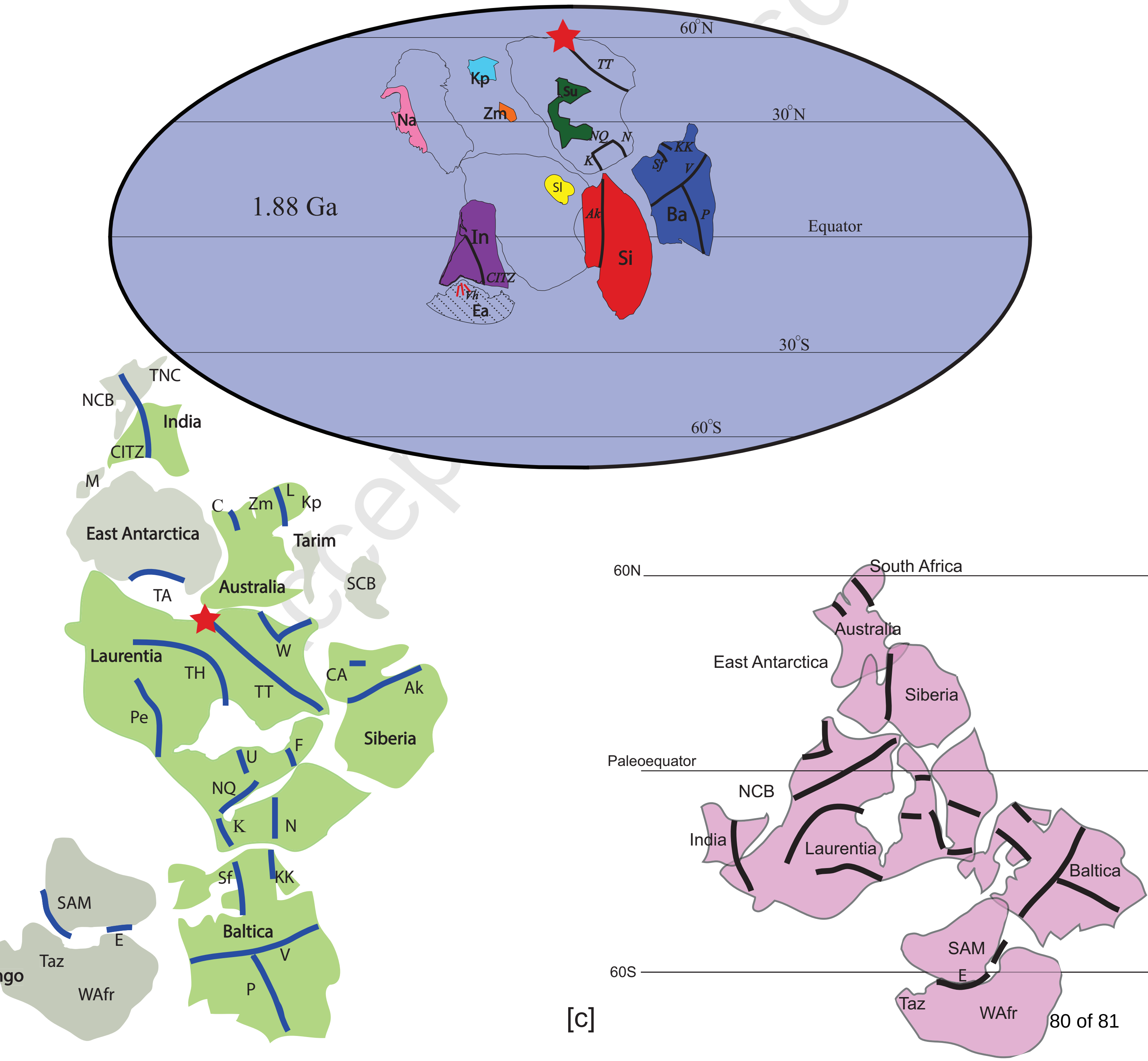

[b]

[c]

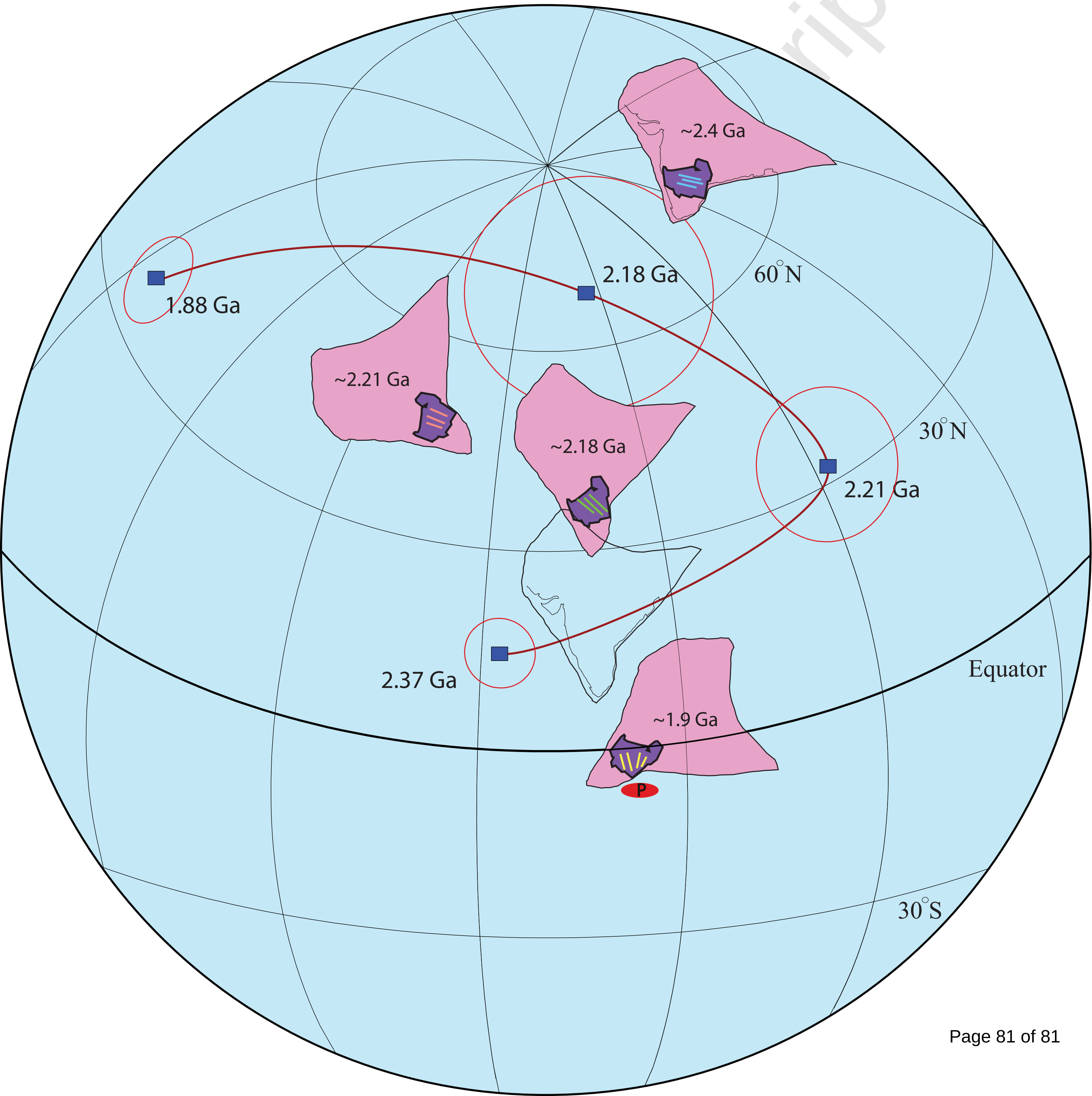
~2.4 Ga
2.18 Ga
60°N
1.88 Ga
~2.21 Ga
~2.18 Ga
30°N
2.21 Ga
2.37 Ga
Equator
~1.9 Ga
P
30°S